L.C.S. Rocha, P. R. Junior, G Aquila, A. Maheri (2022) 'Multiobjective optimization of hybrid wind-photovoltaic plants with battery energy storage system: Current situation and possible regulatory changes', Journal of Energy Storage

MULTIOBJECTIVE OPTIMIZATION OF HYBRID WIND-PHOTOVOLTAIC PLANTS WITH BATTERY ENERGY STORAGE SYSTEM: CURRENT SITUATION AND POSSIBLE REGULATORY CHANGES

Luiz Célio Souza Rocha[1](luiz.rocha@ifnmg.edu.br),
Paulo Rotella Junior[2, *] (paulo.rotella@academico.ufpb.br),
Giancarlo Aquila[3] (giancarlo.aquila@yahoo.com),
Alireza Maheri[4] (alireza.maheri@abdn.ac.uk).

[1] Department of Management, Federal Institute of Education, Science and Technology - North of Minas Gerais, Brazil
[2] Department of Production Engineering, Federal University of Paraiba, Brazil
[3] Institute of Production Engineering and Management - Federal University of Itajuba, Brazil
[4] Centre for Energy Transition, School of Engineering, University of Aberdeen, UK
*Corresponding author

Abstract

The challenges presented by increased electricity generation from intermittent renewable energy sources can be minimized by incorporating energy storage systems (ESS). Despite the benefits, this is still an emerging technology with limited use in Brazil. The aim of the present study is to use a multiobjective optimization process to support the planning of hybrid wind-photovoltaic projects with utility-scale Li-ion battery ESS. Levelised cost of energy (LCOE), diversified energy production density, and net present value are considered as the objectives. The multiobjective optimization is conducted in view of the possible impact of regulatory adjustments necessary for the integration of ESS in the Brazilian context. The optimization problem has been formulated using the mixture arrangement technique and the Normal Boundary Intersection approach is adopted for search in the design space. It is shown that in the current scenario, the possibility of integrating storage reaches only 17.7% of the project capacity. In addition, the investment cost in ESS impacts the viability of the project more than the payout for the service provided. Thus, regulatory adjustments must (i) allow the generation of multiple revenues and avoid double taxation; (ii) predict whether there will be a defined minimum payment for services rendered and/or whether there will be a subsidized credit line; and (iii) develop the production chain that involves storage or create tax incentives for importing equipment to reduce costs. Finally, it is important to highlight that the ESS imposes an increase in the load for the system as a whole and this characteristic needs to be considered for long-term planning.

Keywords: Normal Boundary Intersection; Energy storage market; Electric power quality; Reliability; Flexibility.

1. Introduction

In the past decades, energy consumption has increased significantly due to the economic and population growth [1]. The fastest growth in energy consumption in the last decade was recorded in 2018, with a 2.3% increase in world energy demand [2]. Electricity is the main energy vector nowadays and represents a large energy consumption amount [3], as fossil fuels, due to their negative effects on the environment, cannot be considered a solution to supply the growing demand for energy [4]. One of the main drivers to the electricity sector is the need to shift to cleaner and more diversified electricity production.

Brazil has one of the greatest hydroelectric potentials in the world [5]. However, its dependency on water resources has recently raised questions about the social and environmental

impact of the construction of large dams. Moreover, the prolonged droughts that caused blackouts in 2001 and 2002 led to the discussion on the need` to increase the share of new energy supply sources in the country. Since then, Brazil has liberalized its electricity sector [5] and has created policy schemes to encourage the growth of renewable energy sources (RES) in order to reduce the share of large hydro plants in its energy matrix [6]. After the 2001 and 2002 energy crisis, Brazil was one of the countries that create policy schemes to support RES [7], launching the Incentive Program for Alternative Sources of Electric Energy (PROINFA - from portuguese *Programa de Incentivo às Fontes Alternativas de Energia Elétrica*), aimed to contract 3,300 MW from wind power, small hydro plants, and biomass [8]. In 2014, a drought once again threatened the supply of electricity in Brazil [9]. Low levels of hydro reservoirs led to an increase in energy prices, which further reinforced the need to promote alternatives to hydroelectric dams in Brazil [10].

Due to wind and solar potential, the hybrid wind-solar generation is deemed as a good opportunity to meet the Brazilian electricity demand growth [11]. In contrary to the conventional hydro and thermal plants which provide energy in a constant and predictable manner with precise production scheduling [12], the uncertainties in RES makes it difficult to predict energy production [13]. Biswas et al. [14] state that, generally, wind and solar resource cannot be autonomous in a plant because of their uncertain nature and significant fluctuations in production. Due to the high unpredictability in energy production, means for attaining the power grid stability are required [15,16]. Moreover, a high share of RES results in new challenges to the management of the electricity network, increasing the concern with the reliability of the system [17,18]. One of the current challenges for grid managers is how to combine several sources in a way which provides a better control across the entire distribution system [12].

In Brazil the growth of wind and solar energy in electricity matrix increases the relevance of storage technology [19,20]. The energy storage system (ESS) provides the electrical system with the flexibility required to deal with the fluctuations and intermittent nature of renewable sources. In addition, ESS can accommodate fluctuations in energy demand, mitigating the imbalance between supply and demand. In this way, EES's can improve grid stability and system performance, increase RES integration and reduce the use of fossil fuel energy sources and, consequently, their environmental impacts [1]. In the same sense, Das et al. [21] state that the proper use of the ESS can mitigate some operational challenges related to the use of wind and solar energy, providing voltage regulation, smoothing production fluctuations, balancing the flow of energy in the grid, adjusting supply and demand and helping distribution companies (grid operators and power utilities) to meet demand reliably and sustainably.

Münderlein et al. [22] mention that storage systems such as batteries, supercapacitors, flywheels, pumped hydro energy storage and compressed air energy storage can be used to temporarily store energy for later use. Each of these technologies has different characteristics in terms of round-trip efficiency, cost and lifespan. According to Schmidt et al. [23], pumped hydro energy storage and compressed air energy storage are characterized by relatively slow response times (greater than 10 seconds) and systems with very large minimum sizes (greater than 5 MW), and therefore they are not suitable for fast-response applications such as primary frequency and power quality control, nor for small-scale consumer applications. Flywheels and supercapacitors are characterized by having short duration discharges (less than 1 hour) and are not suitable for applications that require longer-term power supply [23]. Taking all these characteristics into account, the most suitable option is the battery ESS [16,24]. Battery storage is the most appropriate, as it has the necessary power and energy density, as well as an adequate response time [25].The advantages of batteries include greater efficiency, shorter discharge time, and versatility, as it allows mobility, has faster and easier construction, and is easily scalable [26,27]. In recent years, lithium-ion (Li-ion) batteries have become the dominant technology for utility-scale energy storage[28]. Their costs have been drastically reduced and a substantial reduction is expected over the next five to ten years [26, 28–30]. In addition, Li-ion battery technology is considered mature [20], i.e., it reached satisfactory levels of technological

performance, and the possibility of reusing used batteries from electric vehicles favors its future use in the utility-scale energy storage sector [19].

Despite the benefits brought by energy storage, this still remains an emerging technology in Brazil [25]. There is a historical lack of funding for research into storage technologies in Brazil, mainly due to the large hydro system in the country [31]. In fact, the discussion about storage in Brazil was relegated to the background and, therefore, according to Silvera et al. [25], it is difficult to find studies and research works with applications in the Brazilian context. However, this situation is changing and discussions about the regulatory aspects for the energy storage systems (ESS) in Brazil have already started [20]. Due to the variation in generation and the need to balance energy and regulate voltage and frequency, the use of EES's are inevitable in smart grids[25].

Some recent studies on the use of wind and photovoltaic energy in Brazil include the analysis of the economic feasibility of small-scale wind generation [3,9,32], an economic feasibility analysis of small-scale photovoltaic generation [33], optimization of small-scale isolated hybrid systems [34,35], economic feasibility analysis of large-scale wind power plants [6,36], optimization of the configuration of wind power plants [37] and the optimization of large-scale hybrid wind-photovoltaic plants [38,39].None of these studies consider the optimization of the configuration of wind-photovoltaic hybrid plants considering utility-scale battery ESS in Brazil, confirming a literature gap, as previously exposed by Silvera et al. [25] and Dranka and Ferreira [31].

Nowadays, there is no regulation for EES's in-force in Brazil and its financial viability, in the current regulatory configuration, is seen as unlikely [19]. The main barriers for implementation of utility-scale ESS in Brazil are the lack of techno-economic regulation and economic incentives, such as feed-in-tariffs and economic-financial subsidies. Only in 2020, the Brazilian Electricity Regulatory Agency (ANEEL) initiated a Subsidy Taking process, aiming to obtain contributions for regulatory adjustments in the energy storage sector in Brazil. The proposals for regulatory adjustments aim to define the applications of the storage system, in order to define the necessary measures to create a market environment conducive to the inclusion of storage resources in the Brazilian electricity system [20]. In general, it is understood that the regulatory system must evolve to recognize and offset the benefits generated by ESS's [19,20].

Thus, the results of the study reported in this paper become timely in the context of the regulatory adjustments essential for the integration of ESS in the Brazilian National Interconnected System (NIS), and providing information on the economic feasibility of applying this technology in energy projects. Moreover, according to Durusu and Erduman [40], industry investors are looking for methods to minimize installation costs and maximize energy production, targeting rapid growth in the market.

In decisions where only the smallest investment or cost reduction is considered, there is no conflict between two or more objectives and, according to Miettinen [41], no special method is needed. However, when it comes to problems with more than one objective and these objectives are in conflict with each other, it is necessary to use multiobjective optimization methods to solve these problems [42].

Considering the recent interest of investors in wind-photovoltaic hybrid power plants with EES, there is a need to implement mathematical models capable of supporting decision-making to reach the best configuration for these plants, considering the different technical, environmental and economic aspects. More recent studies have discussed the most varied optimization methods in hybrid generation with energy storage in batteries. Abdelkader et al. [43] present a multi-objective optimization using a genetic algorithm for the sizing of distributed generation (photovoltaic and wind) with hybrid ESS. The authors propose the minimization of total cost and the loss power supply probability indicator. Yin et al. [44] propose the optimization of microgrids composed of solar panels, wind turbine and microturbine, in addition to the ESS's. A cost-oriented mathematical model was proposed for sizing and day-ahead resource scheduling problem in energy generation. Tang et al. [45] and Zhao et al. [46], similarly, use different stochastic models for optimization in different climatic

circumstances. In the studies of Yin et al. [44], Tang et al. [45] and Zhao et al. [46], a prioritization approach was used, where the total cost function is minimized, adopting other technical aspects as constraints of the optimization problem. In the present study, a scalarization approach is used instead, in which all objectives are considered in the formulation of the problem allowing the construction of a Pareto frontier.

A multiobjective optimization process, which simultaneously reduces the LCOE, maximizes the diversified energy production density, and produces economically viable solutions is needed to support the planning of hybrid wind-photovoltaic projects with utility-scale Li-ion battery ESS. In this study, the objectives to be optimized are modeled by the mixture arrangement technique with further optimization using the Normal Boundary Intersection (NBI) approach. The final configuration of the hybrid plant is achieved by using Shannon's entropy measure [47].

The financial viability of using ESS's is impacted by issues related to regulatory adjustments. The regulatory framework for energy storage needs to be strategic and long-term [48], because according to Ruester et al. [49], inconsistencies regarding the regulation applicable to the ESS could lead to distortions in competition and inadequate distribution and allocation of resources. This study proposes an optimization routine for utility-scale hybrid generation with battery ESS, contributing to the discussion on the regulatory advances necessary to promote its technical and economic feasibility in Brazil, in addition to promoting discussion about the importance of storage for the modern grid. A discussion is carried out on the policy implications for the construction of a regulatory framework for the utility-scale ESS in Brazil. It is important to highlight that this study does not propose the optimal management of the grid, but the optimal sizing for the investment in utility-scale hybrid plants with battery ESS, considering market scenarios resulting from changes in the regulatory framework.

Considering the current technological level of this sector in the world, the contributions of this study go far beyond the Brazilian case, and the reported policy implications can bring valuable information both for managers of electrical systems in other countries, as well as for others interested in the sector, including especially public policy makers and investors. It is important to highlight that, to the best of our knowledge, there are no studies that specifically use this optimization routine (mixture arrangement, NBI and Shannon's entropy) for studies involving ESS associated with renewable energy generation.

2. Theoretical background

2.1. Experiments with mixtures

Experiments with mixture are the only technique capable of formulating a specific mixture [50]. In the original mixture problem, there is a dependency relationship between the level of the factors [51]. In a mixture problem with p factors, $x_1, x_2, \ldots, x_p$ represent the proportions ($0 \le x_p \le 1$) and,

$$x_1 + x_2 + \ldots + x_p = 1.$$

Simplex-lattice design is the most commonly used method in experimental designing mixture problems. A simplex design with p components and order m has $m + 1$ proportions, evenly spaced from zero to one [51]. Factor levels x_i are obtained as follows:

$$x_i = 0, \frac{1}{m}, \frac{2}{m}, \ldots, 1; \; i = 1, 2, \ldots, p \quad , \tag{1}$$

and, the number of experiments (N) in simplex-lattice is given by:

$$N = \frac{(p + m - 1)!}{m!(p - 1)!} \tag{2}$$

An alternative to simplex-lattice is the simplex-centroid. For this case, the *k* input variables are set in $2^k - 1$ points, corresponding to *k* permutations of (1, 0, 0, ..., 0), to $\binom{k}{2}$ permutations of $\left(\frac{1}{2},\frac{1}{2},0,...,0\right)$, to $\binom{k}{3}$ permutations of $\left(\frac{1}{3},\frac{1}{3},\frac{1}{3},0,...,0\right)$ and the centroid $\left(\frac{1}{k},\frac{1}{k},...,\frac{1}{k}\right)$ [51].

A disadvantage of simplex design is due to the fact that most experiments take place at the boundaries of the arrangement and only few points in the inner part are tested. Thus, it is recommended, whenever possible, to increase the number of experiments by adding internal points to the arrangements, such as the center points and also the axial points. Axial points could be defined as all permutations of $((k+1)/2k,\ 1/2k,\ \ldots,\ 1/2k)$, where *k* is the number of input variables. In the case of mixture arrangements, it is worth noting that the center points correspond to the centroid itself.

As for the mathematical models used to represent the responses, it appears that the mixture models present some differences in relation to the standard polynomials used in the response surface methodology, mainly due to the existence of the constraint function $x_1 + x_2 + \ldots + x_p = 1$. If β_0 is multiplied by $x_1 + x_2 + \ldots + x_p = 1$ in a first-order model, the following is generated:

$$E(y) = \beta_0 + \sum_{i=1}^{q} \beta_i x_i = \beta_0 (x_1 + x_2 + \ldots + x_q) + \sum_{i=1}^{q} \beta_i x_i = \sum_{i=1}^{q} \beta_i^{canonical} x_i \qquad (3)$$

where $\beta_i^{canonical} = \beta_0 + \beta_i$

This is called the canonical form of the first-order mixture model [52].

2.2. Multiobjective Optimization

In modern energy planning process, the models are becoming more complex, being necessary to consider technical, environmental and economic attributes. In this sense, models that consider only the minimization of costs are unrealistic [53]. To deal with these more complex models, and therefore more realistic, it is necessary to formulate a multiobjective optimization problem, in order to find Pareto optimal or non-dominated solutions. A general multiobjective optimization problem can be demonstrated as [42]:

$$\begin{aligned} &Min.\ \{f_1(x), f_2(x), ..., f_k(x)\} \\ &s.t.:\ h_i(x) = 0,\ i = 1, 2, ..., l \\ &\quad g_j(x) \le 0,\ j = 1, 2, ..., m \end{aligned} \qquad (4)$$

where: $f_1(x)$, $f_2(x)$,...,$f_k(x)$ are objective functions to be optimized; $h_i(x)$ represents the *l* equality constraints; and $g_j(x)$ represents the *m* inequality constraints.

The most used approach to generate Pareto optimal solutions in multiobjective optimization problems is the weighted sums method since this is a simple method to be implemented and clearly represents a physical interpretation of the analyzed problem [54]. However, the weighted sums method does not work well for problems involving non-convex equations and cannot produce a uniformly distributed Pareto frontier, even for convex problems [55].

To avoid these problems (convexity constraint of equations and non-uniform distribution of points on the Pareto frontier), the NBI method was proposed [56]:

$$\underset{(x,\,D)}{Max.}\ D$$

$$s.t.:\ \bar{\Phi}(w-De)=\bar{F}(\mathbf{x})\therefore\begin{bmatrix}\dfrac{f_1^*(x_1^*)-f_1^*(x_1^*)}{f_1(x_m^*)-f_1^*(x_1^*)} & \cdots & \dfrac{f_1(x_m^*)-f_1^*(x_1^*)}{f_1(x_m^*)-f_1^*(x_1^*)}\\ \vdots & \ddots & \vdots\\ \dfrac{f_m(x_1^*)-f_m^*(x_m^*)}{f_m(x_1^*)-f_m^*(x_m^*)} & \cdots & \dfrac{f_m^*(x_m^*)-f_m^*(x_m^*)}{f_m(x_1^*)-f_m^*(x_m^*)}\end{bmatrix}(w-De)=\bar{F}(\mathbf{x}) \quad (5)$$

$$\mathbf{x}\in\Omega$$

where: *D*is the distance from the Pareto frontier to the utopia line; $\bar{\Phi}$ is the normalized payoff matrix; *w* is the weighting; *e* is a vector of value 1; and $\bar{F}(\mathbf{x})$ is the vector containing the individual values of the normalized objectives functions.

Shannon's entropy measure[47] is used to identify the best solution within the Pareto frontier. The maximization of the Shannon's entropy measure is carried out in order to diversify as much as possible the composition of the hybrid project under analysis. Rocha et al. [42,54,57–59] demonstrated that the use of this type of metric reduces the prediction variance of the obtained response. Shannon's entropy can be calculated as:

$$S(x)=-\sum_{i=1}^{m}x_i\ln x_i \quad (6)$$

where: x_i represents the decision variables of the functions to be optimized, being the proportions of wind, solar photovoltaic and storage systems used in the plant.

2.3. Objectives to be optimized

The objectives to be optimized include socio-environmental and economic-financial issues related to the implementation of a hybrid wind-photovoltaic plant with ESS in utility-scale batteries.

2.3.1. Diversified Energy Production Density

The energy density produced by a hybrid wind-photovoltaic plant with utility-scale battery ESS corresponds to the amount of produced electricity per area during a given period, and when maximized, contributes to the well-being of the electricity sector. The calculation of energy production density can be described mathematically, according to Equation 7:

$$\rho_e=\frac{TEP}{A} \quad (7)$$

where, ρ_e is the energy production density (kWh/m^2), *TEP* is the total energy produced over the lifespan of the project (kWh), *A* is the occupied area (m^2).

The total electricity produced over the lifespan of the project (*TEP*) can be determined by the sum of the total electricity produced per year (*AEP*) adjusted by the degradation rate (φ) during the project duration and brought to current date:

$$TEP=\sum_{t=0}^{n}\frac{AEP_{adj.}}{(1+i)^t} \quad (8)$$

where,: *n* is a given year of the project's lifespan, $AEP_{adj.}$ is the adjusted *AEP*, according to Equation 15 below, *t* is the time in years, and *i* is the real discount rate, represented by the Weighted Average Cost of Capital (WACC), discounting by inflation.

The *AEP* estimate in kWh per year, is given by Equation 9. It is obtained from the sum of wind and photovoltaic energy, associated with the energy demand generated by the ESS, since this type of system consumes more energy than the amount actually returned to the grid.

$$AEP=PVe+We-Be \quad (9)$$

where, *PVe* is the photovoltaic energy produced per year, *We* is the wind energy produced per year, *Be* is the energy deficit which is supplied by the ESS per year.

The tendency is for the *AEP* estimate to decrease over time, as the equipment degrades. According to Rocha et al. [33], in order to calculate the energy produced by an energy systems, the degradation rate (φ) for each system's component must be considered. The adjusted *AEP* ($AEP_{adj.}$) in a given year is given by:

$$AEP_{adj.} = AEP\ (1-\varphi)^n \tag{10}$$

where, φ is the degradation rate per year; and *n* is a given year of the useful life of the equipment.

The production of photovoltaic energy depends on the level of insolation as well as the temperature [60]. To calculate the production of photovoltaic energy, the irradiance level data, in kW/m², at each hour of the day for each month of the year, relative to the place of analysis will be necessary. Equation 11 presents the calculation of the power generated by the photovoltaic panels.

$$P = \eta_{PV} \times I_m \times A \times \left(1 - \Delta T \times \theta_T\right) \tag{11}$$

where, *P* is the generated power (kW), η_{PV} is the efficiency of photovoltaic panels (dimensionless), I_m is the irradiance (kW/m²), *A* is the area of photovoltaic panels (m²), ΔT is the temperature difference above the cell standard temperature (normally 25ºC), and θ_T is the temperature loss coefficient.

With the power of the panels, it is possible to estimate the amount of energy produced by the equipment in a given period. Equation 12 presents the calculation for energy production.

$$E = P \times t \tag{12}$$

where: *E* is the amount of electricity produced (kWh); *P* is the generated power (kW); and *t* is the hourly insolation.

In calculating the annual generation of photovoltaic energy, the simulated hourly productions for each year will simply be added, as can be seen in Equation 13[33]:

$$PVe = \sum E(t) \tag{13}$$

where, *PVe* is the photovoltaic energy produced per year (kWh)

To estimate the energy production of each wind turbine used in this study, a regression model for the power curve is estimated, considering wind speed as an independent term. The data used are provided by the manufacturer of the wind turbines. Thus, a fifth-degree polynomial interpolation is chosen for the turbine power curves (Equation 14).

$$\begin{cases} P = \beta_0 + \beta_1 v^1 + \beta_2 v^2 + \beta_3 v^3 + \beta_4 v^4 + \beta_5 v^5, \text{if } v < v_{max} \\ P = P_{max}, \text{if } v \geq v_{max} \end{cases} \tag{14}$$

where, *P* is the generated power (kW), β_i are the coefficients of the equation, *v* is the wind speed, v_{max} is the maximum speed defined by the manufacturer from which the generated power is constant, and P_{max} is the maximum power generated by the wind turbine.

The hourly wind speed data will be used for the analyzed site, so 8760 (365 days × 24 hours) hourly energy generation calculations per year will be employed. The sum of these data is equivalent to the annual wind energy generation, from which the losses related to the generator and transmission systems will also be discounted, according to Equation 15:

$$We = \sum E(t)\eta_W \tag{15}$$

where, *We* is the wind energy produced per year (kWh), *E* is the amount of hourly electricity produced by the turbine rotor (kWh), and η_W is the combined electrical-mechanical efficiency of the wind turbine, calculated as ~~(1 - %losses)~~.

It is important to highlight that the wind speed data will be corrected for the height of the wind turbine hub through the power law given by Equation 16 [61]:

$$v_2 = v_1\left(\frac{h_2}{h_1}\right)^{\alpha} \tag{16}$$

where, v_2 is the projected wind speed at the desired height h_2, v_1 is the wind speed measured in height h_1, α is the dimensionless exponent of wind shear.

In the case of utility-scale battery ESS, the logic is inverted, as the system absorbs more energy from the grid than is actually returned, generating a deficit in production. Thus, the amount of energy delivered by a utility-scale battery ESS can be calculated by Equation 17, obtained from modifications to the data presented in Rahman et al. [62]:

$$E_{delivered} = P \times t \times \eta_{battery} \times DOD \times NC \times \eta_{PCS} \tag{17}$$

where, $E_{delivered}$ is the amount of electricity (kWh) fed into the grid by the ESS in one year, *P* is the nominal capacity of the battery bank (kW), *t* is the duration of the discharge (hours), $\eta_{battery}$ is the round-trip efficiency, *DOD* is the depth of discharge (-), *NC* is the number of cycles in a year; and η_{PCS} is the power conversion system efficiency.

The amount of electricity received from the grid by the utility-scale battery ESS can be calculated by Equation 18, also modified from Rahman et al. [62]:

$$E_{charged} = \left(\frac{P \times t \times \eta_{battery} \times DOD}{\eta_{battery} \times \eta_{PCS}}\right) \times NC \tag{18}$$

where, $E_{charged}$ is the amount of energy (kWh) required to charge the ESS for one year.

The annual energy deficit (kWh) generated due to the ESS operation, *Be* can be defined as:

$$Be = E_{charged} - E_{delivered} \tag{19}$$

In the present study, self-discharge losses are not included as they are anticipated to be less than 0.06% per day [63,64]. A similar strategy has been used by other authors [62, 63, 65].

With the energy production data from different sources, the energy consumption of the ESS and the respective areas necessary for the implementation of each technology, it is then possible to calculate the energy production density (ρ_e), as given by Equation 7.

Based on modifications in studies by Stirling [66–68], the energy production density metric will be associated with a diversification metric as shown in the following equation:

$$\rho_e \Delta = \sum_{ij(i \neq j)} \rho_e (w_i w_j) \tag{20}$$

where, $\rho_e \Delta$ is the diversified energy production density metric, and w_i and w_j are the weights assigned to each technology in a given project.

The diversified energy production density metric, when maximized, ensures maximum energy production per occupied area and maximum diversification among the technologies involved in the project under analysis.

2.3.2. Levelized Cost of Energy

The Levelized Cost of Energy (LCOE) is a metric widely used to assess generation costs from different technologies and energy sources. According to Aquila et al. [38], this method relates the total energy generation cost with the total energy produced during the system lifespan. The total cost includes all expenses directly related to energy production, namely, total investment cost, operating and maintenance (O&M) cost, interest payment, sector charges, and taxes.

In projects which incorporate utility-scale battery ESS, the cost of charging the batteries as well as the cost of replacing the equipment over the life of the project must also be considered. Although the literature presents different names for this metric when associated with storage, such as LCOS (levelized cost of storage), for example, it is decided to keep the more comprehensive name, LCOE.

$$LCOE = \frac{\sum_{t=0}^{n} \frac{C_t}{(1+i)^t}}{\sum_{t=0}^{n} \frac{Ep_t}{(1+i)^t}} \quad (21)$$

where, C_t stands for the total cost of energy generation, including the cost of storage, operation and maintenance, replacement, and subtracted the residual or salvage value, in a given period t, t is the time in years, Ep_t is electricity production of the plant in each period t and is equivalent to $AEP_{adj.}$ as described in Equation 10, and i is the deflated discount rate.

The methodology used to determine the discount rate in the LCOE is the Weighted Average Cost of Capital (WACC). According to Rocha et al. [33], the WACC is obtained by:

$$WACC = k_d D(1-\tau) + k_e E \quad (22)$$

where, k_d is the cost of debt, D is the debt amount to support the investment (%), τ is the income tax rate (%), k_e is the cost of equity, and E is the equity applied in the investment (%).

The Capital Asset Pricing Model (CAPM) model presented by Sharpe [69] is adopted for calculating cost of equity capital. As applied in Aquila et al. [70] and Stetter et al. [71], and presented in Steffen [72], the following equation is used:

$$k_e = r_f + \beta \times (r_m - r_f) \quad (23)$$

where, r_f is the risk-free rate (%), β is the leveraged beta and measures the project risk in relation to the market, and $(r_m - r_f)$ is the market risk premium (%).

The leveraged β is calculated from the unlevered β of the renewable energy sector presented in Aquila et al. [70]. The procedure for obtaining the leveraged beta is presented in Equation 24 [73]:

$$\beta = \beta_{unlevered}\left(1 + {}^{D}\!/\!_{E}\right)(1-\tau) \quad (24)$$

where, τ is the income tax rate (%).

Once the discount rate is obtained, it can be deflated using the main Brazilian inflation index called the Broad Consumer Price National Index (IPCA, from portuguese *Índice Nacional de Preços ao Consumidor Amplo*). This process is necessary, as price changes resulting from inflation will not be considered in the project annual cash flow. Equation 25 presents the process for deflating the discount rate:

$$i = \frac{(1+WACC)}{(1+IPCA)} - 1 \quad (25)$$

2.3.3. Net Present Value

The economic feasibility analysis indicates if an investment is economic attractive or not. Among the available criteria, the most used in literature studies involving the financial analysis of RES plants is the Net Present Value (NPV). The literature on financial management emphasizes that an investment must be considered when the NPV is greater than or equal to zero[74]. The equation for calculating the NPV is:

$$NPV = \sum_{t=0}^{n} \frac{CF_t}{(1+i)^t} \quad (26)$$

where, i is the deflated discount rate, t is the time in years, and CF_t is the net cash flow in the year t.

As in the case of the LCOE, the WACC will be used to determine the discount rate, which will later be deflated.

3. Methodology

The general objective of this study is to propose an optimization method for the configuration of wind-photovoltaic hybrid power plant projects with utility-scale battery storage systems while considering the possible impact of regulatory adjustments for the inclusion of ESS in the Brazilian context. A project of a hybrid wind-photovoltaic plant with ESS with a total installed capacity of 60 MW is considered as the case. The percentages of the amount of wind energy, solar energy and the storage in the project are the input variables (x_i), and the performance measures LCOE, diversified energy production density and NPV are calculated for each plant configuration, defined by the experimental arrangement.

The present study is expected to contribute to the discussion on the use of utility-scale battery storage system, a technology that is little used in Brazil. The optimization of the configuration of plants with these characteristics for the Brazilian scenario will enable the discussion of their economic viability, in the current situation and given the regulatory adjustments necessary for the implementation of ESS in the NIS, hence allowing (i) the definition of the optimal configuration of hybrid wind-photovoltaic plants with utility-scale battery ESS, (ii) analysis of the economic viability considering the lack of regulation for ESS, and (iii) elaborating on how the regulatory aspects could affect the economic viability of using ESS.

This study will follow the following steps:

1. Generate the experimental conditions from the levels of the decision variables (x_i), which will be the percentages of the amount of wind energy, solar energy and storage.

2. Calculate the responses (y_i) - LCOE, diversified energy production density and NPV - from the experimental arrangement.

3. Mathematically model the responses (y_i) as functions of the percentages of different technologies (wind, solar, storage) implemented in the project.

4. Optimize the multiobjective problem.

5. Discuss the regulatory adjustments necessary for the integration of ESS in the Brazilian context.

In order to model the objective functions of the present study (LCOE, diversified energy production density and NPV), experiments will be generated using the mixture design methodology, using a level 4 simplex-lattice, and the percentage proportions of wind source, solar source and storage as input variables (x_i) in the model. Table 1 presents the experimental design.

Table 1 – Experimental design

Experiment number	Wind		Solar		ESS		Sum	
	%	MW	%	MW	%	MW	%	MW
1	100	60	0	0	0	0	100	60
2	75	45	25	15	0	0	100	60
3	75	45	0	0	25	15	100	60
4	50	30	50	30	0	0	100	60
5	50	30	25	15	25	15	100	60
6	50	30	0	0	50	30	100	60
7	25	15	75	45	0	0	100	60
8	25	15	50	30	25	15	100	60
9	25	15	25	15	50	30	100	60
10	25	15	0	0	75	45	100	60
11	0	0	100	60	0	0	100	60
12	0	0	75	45	25	15	100	60

13	0	0	50	30	50	30	100	60
14	0	0	25	15	75	45	100	60
15	0	0	0	0	100	60	100	60
16	33.3	20	33.3	20	33.3	20	100	60
17	66.7	40	16.7	10	16.7	10	100	60
18	16.7	10	66.7	40	16.7	10	100	60
19	16.7	10	16.7	10	66.7	40	100	60

After mathematical modeling of the objective functions, the NBI method is used for multiobjective optimization. For the purposes of this study, NPV is minimized with a greater than or equal to zero constraint, to ensure minimum viability to the investor, while avoiding a high transfer of investment cost in these systems to the final consumer. The LCOE is minimized, while the diversified energy production density response ($\rho_e \Delta$) is maximized. To perform statistical analysis, mathematical modeling, simulations and optimization, software tools Solver®, Minitab® and Statistica® are used.

Caetité in Bahia, a city with high potential of wind speed and solar irradiation is chosen for the present study.

3.1. Renewable resources: wind speed and solar irradiation

The wind speed and solar irradiation are obtained from the Solar and Wind Energy Resource Assessment [75]. The maximum average temperature data for the location under study are obtained from the National Institute for Space Research [76].

Tables A1, A2 and A3 present, respectively, the monthly solar irradiation, maximum average temperatures and wind speed data, at a height of 100 meters (see Appendix A). In order to compare the behavior of solar irradiation and wind speed in each month, Figures 1 and 2 resume the data presented in Tables A1 and A3, respectively.

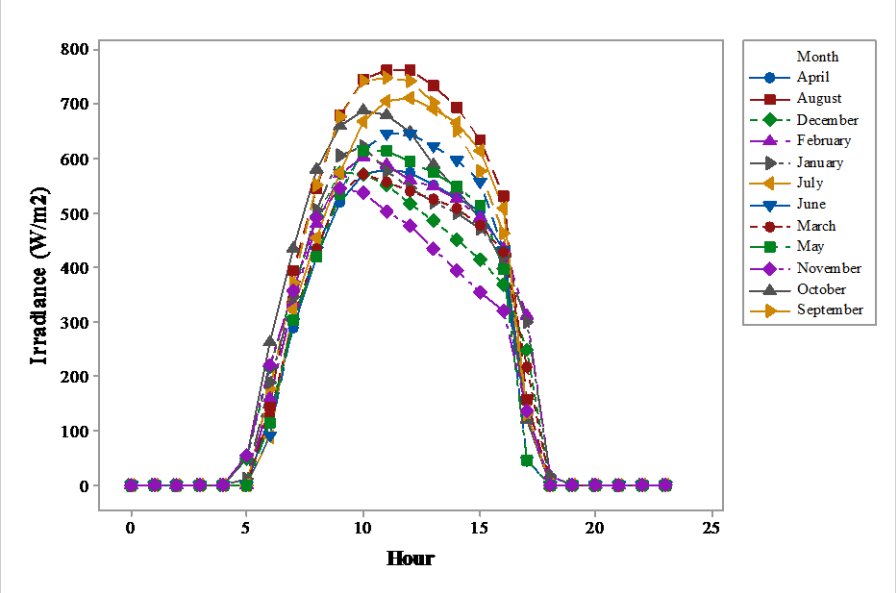

Figure 1 - Irradiation data (Wh/m^2) from Caetité-BA

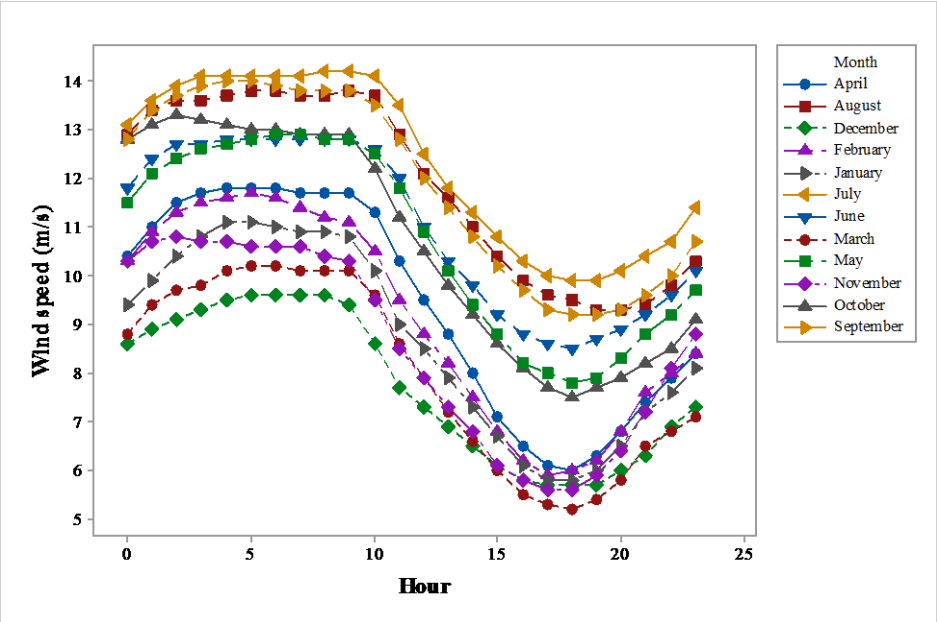

Figure 2 - Wind speed data (m/s) from Caetité-BA

Figures 1 and 2 show that the months of July, August and September are the months with the best conditions for wind speed and irradiation, coinciding with the months with the lowest levels of precipitation in Brazil (especially July and August). This is an argument in favor of investing in energy production from these sources, aiming at diversifying the Brazilian electricity matrix. Another argument in favor of hybrid plants is the complementarity of energy production between these sources, as, at the time of day when energy production from wind sources starts to decline, solar production reaches its peak, as shown in Figure 3.

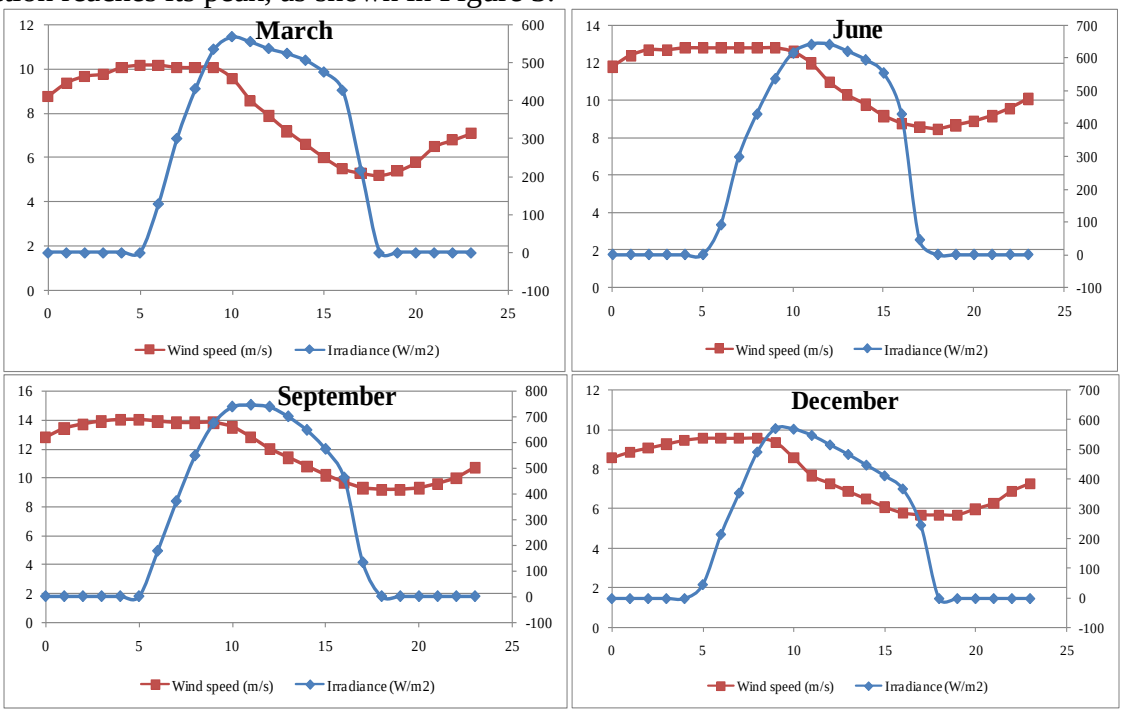

Figure 3 - Complementary behavior between wind and solar sources in Caetité-BA

3.2. Assumptions for Electric Power Generation Models

For the calculations related to solar photovoltaic energy production, the following data are used [77]: nominal cell power of 320 W; efficiency of photovoltaic panels (η_{PV}) of 19.6%; irradiation

(kWh), which is equal to the calculation of irradiance (I_m) times time (t), as shown in Table A1; area of photovoltaic panels (A) equal to 1.94 m^2; and temperature loss coefficient (θ_T) of 0.39 %/ºC for temperatures above 25ºC. The number of photovoltaic cells to be used is defined by dividing the installed capacity of photovoltaic solar energy in each experimental condition by the nominal power of the cell, which is 320 W.

The wind turbines manufacturer data [78] are used to generate the power curve regression models. Table B1 (in Appendix B) presents the mathematical models for different wind turbines used in this study and Figure 4 shows the mathematical models and the manufacturer data.

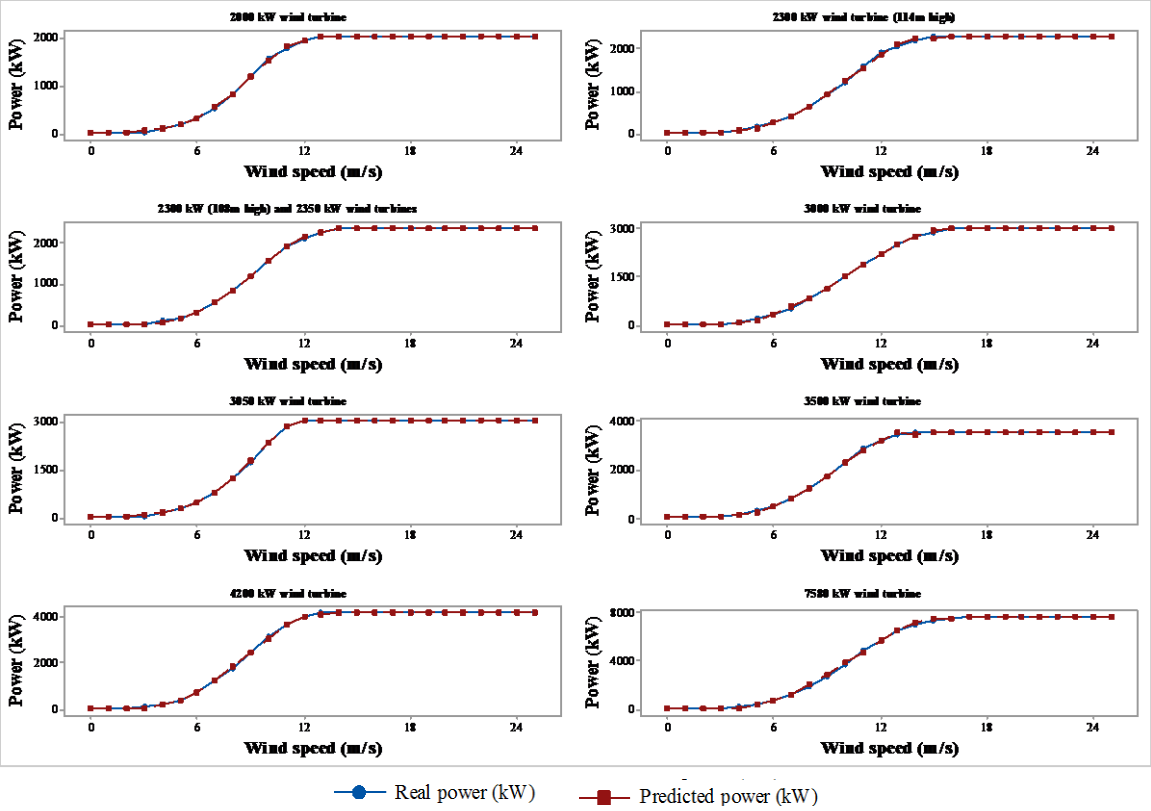

Figure 4 - Power data (real x estimated)

The efficiency of wind turbines (η_W) considered in this study is 91.0% [3, 38]. In order to adjust the wind speed at the hub height of the wind turbines, an α (dimensionless exponent of wind shear) of 0.25 corresponding to a flat terrain with low to moderate vegetation is used [61].

For the utility-scale battery ESS the following data are used: discharge duration time of 4 hours; battery round-trip efficiency of 90% [79]; one cycle of charge-discharge per day [62] with a depth of discharge of 80% [80]; and a power conversion system efficiency of 95% [81]. To determine the number of cycles of a Li-ion battery in its useful life Equation 27 [82] is used.

$$CL = 2731.7 \times (DOD)^{-0.679} \times e^{\left[1.614 \times (1-DOD)\right]} \quad (27)$$

where, CL is the number of cycles during battery life and DOD is depth of discharge.

The annual degradation rates (φ) for each type of equipment, there following values used: 0.57% for the wind farm [83]; 0.60% for the photovoltaic solar plant [84]; and 0.50% for ESS [85].

The areas occupied by each technology are: 28,571.43 m^2/MW for photovoltaic energy (calculated from data presented in Hernandez et al. [86]); 431,499.00 m^2/MW for wind energy (calculated from data presented in Lovins [87], Denholm et al. [88]); and 118.92 m^2/MW for batteries (calculated from data presented in Fu et al. [89]).

The monthly energy production from each source is shown in Figure 5. It is important to note that the calculated capacity factors for the wind and solar photovoltaic projects are 54.93% and 27.76%, respectively, which are very close to the values reported for the region under analysis [90,91]. The average monthly deficit of energy production, or simply energy consumption, of the battery ESS is 1,154.17 MWh, being calculated through Equation 19.

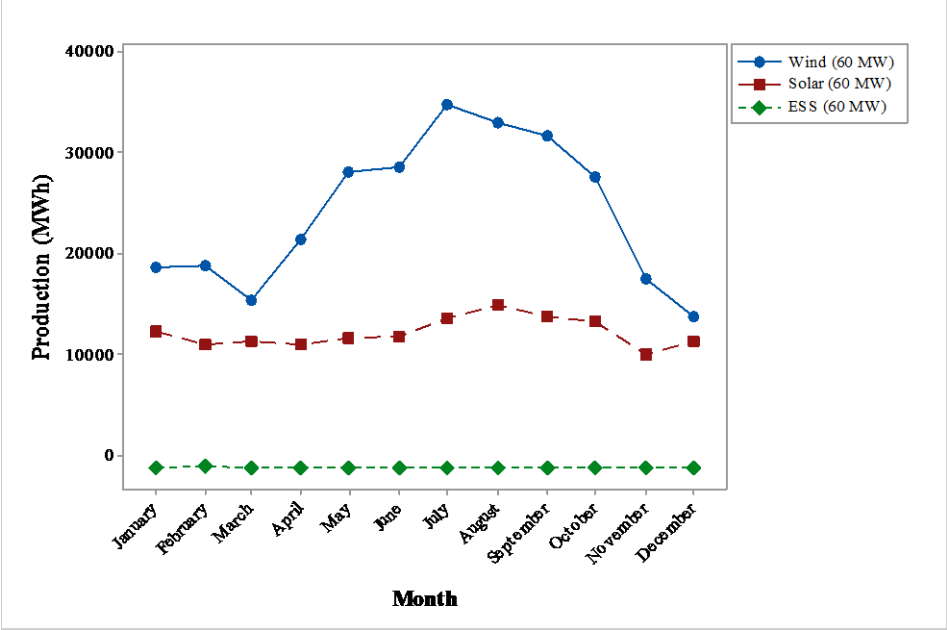

Figure 5 - Monthly energy production

Using Equation 7, the energy production density can be calculated. The energy production density values for all-wind, solar photovoltaic and ESS projects are 0.1519 MWh/m^2, 1.1562 MWh/m^2 and, -27.1164MWh/m^2, respectively. Solar energy generation technology has a lower capacity factor than wind generation, but with greater efficiency in terms of electrical production per occupied area. The ESS, on the other hand, has an excellent energy capacity per occupied area.

3.3. Assumptions for financial analysis models

Table C1 (Appendix C) shows the assumptions used in this study for the financial analysis of the project, represented by LCOE and NPV.

The current ESS investment cost is obtained from an average of the values reported by Rahman et al. [62], Cole and Frazier [92] and Fu et al. [89], resulting R$ 7,788,733.33/MW (rounded to R$ 8,000,000.00/MW). The ideal ESS investment cost is presented by Penisa et al. [93] as US$100.00/kWh, which results in US$400.00/kW for 4-hour batteries. This amount, after conversion and rounding, generated the amount of R$ 2,000,000.00/MW. For the payout for the services provided by the ESS, the value of R$ 0.00/MWh is adopted for the current situation, due to the lack of regulation, and the value of R$ 380.12/MWh is adopted for the ideal payout, based on the value of US$ 68.00/MWh presented by Davies et al. [94], assuming that the practice of generating multiple revenues or stacking of revenues is allowed.

4. Results and discussion

As mentioned before, Brazil currently does not have any in force regulations for the use of energy storage. Hence, in the current scenario there is no payout for the energy storage service provided by any agent in the electricity market. In addition, investment costs are considerably high due to the lack of an industry focused on serving the energy storage sector in Brazil. Based on these premises, scenarios are created in order to represent the current situation and a possible ideal situation from the implementation of public policies and regulatory framework for the energy sector in Brazil.

The analysis of the proposed scenarios allows the presentation of a discussion about the possible governmental incentives.

Based on the current and ideal ESS investment costs and the current and ideal ESS payout level, four analysis scenarios are generated: (a) Scenario 1 considers an investment cost in ESS of R$ 2,000,000 per installed MW (ideal) with payout for storage of R$ 0.00 per MWh (current); (b) Scenario 2 considers an ESS investment cost of R$ 8,000,000 per installed MW (current) with payout for storage of R$ 0.00 per MWh (current); (c) Scenario 3 considers an ESS investment cost of R$ 2,000,000 per installed MW (ideal) with payout for storage of R$ 380.12 per MWh (ideal); and (d) Scenario 4 considers an ESS investment cost of R$ 8,000,000 per installed MW (current) with payout for storage of R$ 380.12 per MWh (ideal). The comparative analysis of these scenarios will give us indications of how the investment costs and ESS payout impact the implementation of this technology in the Brazilian context.

4.1. Results for Scenario 1

Based on the initial conditions stipulated in relation to the ESS for Scenario 1 (investment of R$ 2,000,000 per MW installed with payout for storage of R$ 0.00 per MWh), the values of the response variables (y_i) NPV, LCOE and diversified energy production density are calculated, for the entire experimental arrangement, as shown in Table 2.

Table 2–Experimental arrangement - Scenario 1

N	Wind (%)	Solar (%)	ESS (%)	NPV (R$)	LCOE (R$/MWh)	$\rho_e \Delta$ (dimensionless)
1	1.000	0.000	0.000	317,834,128.48	108.18	0.000
2	0.750	0.250	0.000	243,949,569.68	119.67	0.032
3	0.750	0,000	0.250	148,195,975.81	128.23	0.027
4	0.500	0.500	0.000	185,237,478.18	132.05	0.053
5	0.500	0.250	0.250	89,483,884.31	143.50	0.055
6	0.500	0.000	0.500	-6,269,709.56	157.77	0.035
7	0.250	0.750	0.000	129,139,448.93	148.39	0.059
8	0.250	0.500	0.250	33,385,855.07	164.43	0.081
9	0.250	0.250	0.500	-62,367,738.80	185.36	0.062
10	0.250	0.000	0.750	-158,121,332.67	213.84	0.024
11	0,000	1.000	0.000	71,347,361.75	173.00	0.000
12	0,000	0.750	0.250	-24,406,232.12	197.60	0.209
13	0,000	0.500	0.500	-120,159,825.99	232.19	0.260
14	0,000	0.250	0.750	-215,913,419.86	284.41	0.151
15	0,00	0.000	1.000	-312,009,957.22	372.77	0.000
16	0.333	0.333	0.333	25,819,039.27	159.97	0.069
17	0.667	0.167	0.167	165,964,646.25	128.28	0.041
18	0.167	0.667	0.167	48,583,200.51	166.07	0.089
19	0.167	0.167	0.667	-142,923,987.23	217.55	0.047

The data presented in Table 2 are used to generate the equations for NPV (y_1), LCOE (y_2) and diversified energy production density (y_3) as a function of the proportions of each technology considered (x_i). The mathematical models can be seen in Table 3. The adequacy of the models is analyzed by ANOVA. The p-values for the objective functions under analysis show a statistically significant regression at the 5% significance level, proving the adequacy of the functions. Also, the values of R^2 and R^2 adjusted show that the models have a good fit.

Table 3–Mathematical models for objective functions - Scenario 1

Terms	NPV (R$)	LCOE (R$/MWh)	$\rho_e \Delta$ (dimensionless)
% Wind	**313,142,811.338**	**118.044**	**0.002**
% Solar	**71,655,963.520**	**174.106**	**0.013**
% ESS	**-311,589,249.372**	**356.884**	**-0.020**
% Wind x *% Solar*	-22,503,448.690	-46.695	**0.209**
% Wind x *% ESS*	-21,909,269.001	**-336.860**	**0.178**
% Solar x *% ESS*	8,303,413.778	**-137.975**	**0.984**
% Wind x *% Solar* x *% ESS*	-	-	**-2.453**
p-value	0.000	0.000	0.000
R^2 (%)	99.97%	98.13%	95.08%
R^2adjusted (%)	99.96%	97.40%	92.61%

Values in bold represent significant terms in the models (p-value< 5%).

Figures 6, 7 and 8 are the graphical representations of the mathematical models presented in Table 3, i.e., NPV (y_1), LCOE (y_2) and diversified energy production density (y_3) respectively. These models have %Wind (x_1), %Solar (x_2) and %ESS (x_3) as decision variables. The vertices in these figures represent the responses of a power generation project with 100% of a given source. The response surface and the counter plot are different perspectives for the same mathematical model, representing the values of NPV (y_1), LCOE (y_2) and diversified energy production density (y_3), for each different combination of decision variables.

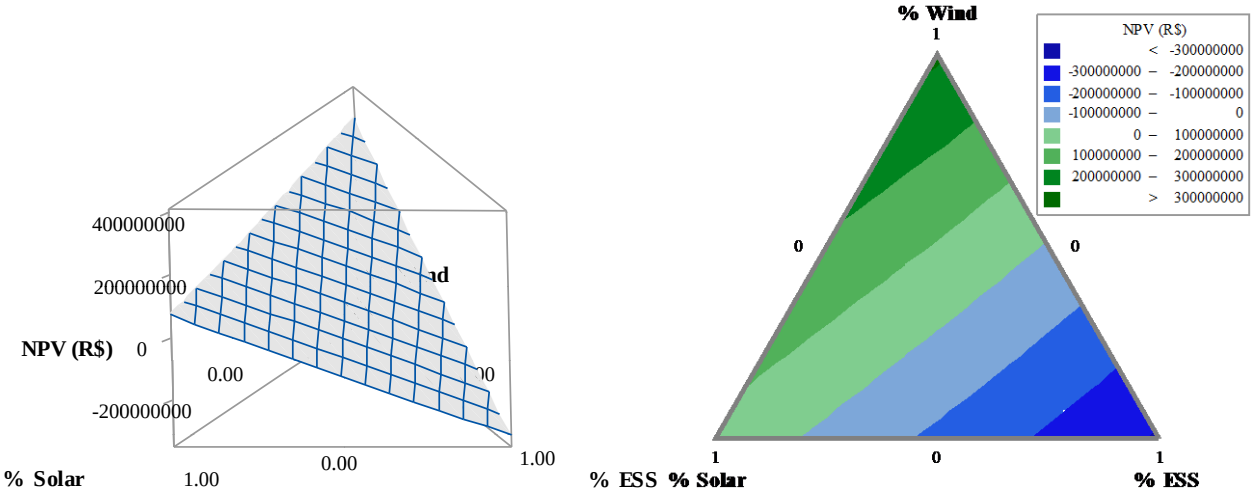

Figure 6 – Response surface and Contour plot for NPV - Scenario 1.

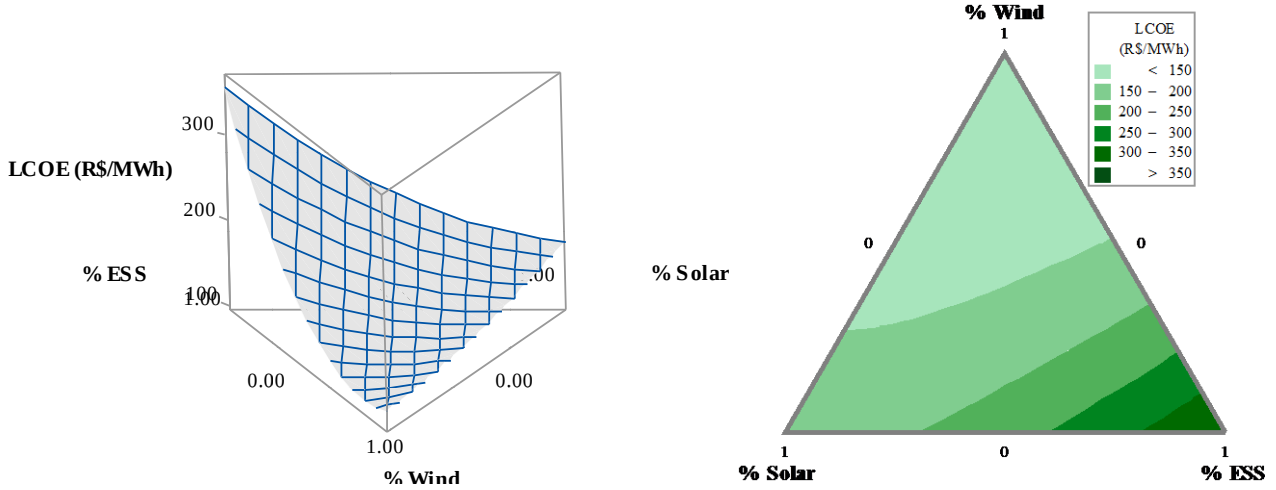

Figure 7 – Response surface and Contour plot for LCOE - Scenario 1.

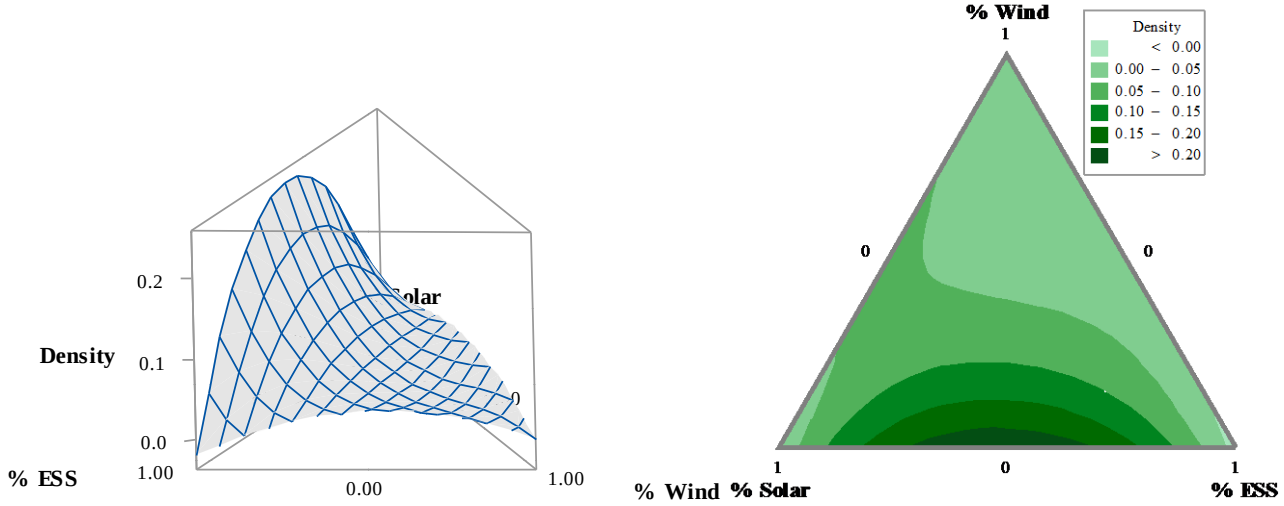

Figure 8 – Response Surface and Contour plot for Diversified Energy Production Density - Scenario 1.

To implement the NBI optimization process, the payoff matrix is initially estimated, obtaining the results shown in Table 4. In order to define the configuration of a hybrid plant that would allow the integration of the ESS while maintaining the viability of the project, (a NPV greater than or equal to zero), the minimization of the NPV function is adopted. The LCOE function also is minimized, seeking to minimize cost, while the diversified energy production density response ($\rho_e \Delta$) is maximized.

Table 4–Payoff matrix for objective functions - Scenario 1

NPV (R$)	LCOE (R$/MWh)	$\rho_e \Delta$ (dimensionless)
-311,589,249.37	356.88	-0.020
219,526,230.77	**110.91**	0.021
-111,491,143.52	227.99	**0.243**

Note: values in bold represent individual optimum.

NBI methodology is used to solve the multiobjective optimization problem. Therefore, weights (w_i) are assigned to NPV (y_1), LCOE (y_2) and diversified energy production density(y_3). By using values for w_i with step size of 0.20 bounded in the interval [0 1], 21 points are generated. These points are in addition to three axial points (combinations of weights 0.667, 0.167 and 0.167) and one central point (w_1, w_2 and w_3 equal to 0.333), totaling 25 points. Thus, it is possible to obtain the Pareto optimal solutionsfor each combination of weights, as presented in Table 5. When changing the degree

of importance attributed to each response, the results of the optimization process are changed, favoring the response with greater weight [95]. Figure 9 graphically presents the obtained Pareto Frontier.

Table 5–Pareto Optimal Set - Scenario 1

Weights			*% Wind*	*% Solar*	*% ESS*	NPV (R$)	LCOE	$\rho_e \Delta$	Entropy
w_1	w_2	w_3	(x_1)	(x_2)	(x_3)		(R$/MWh)	(dimensionless)	
1.000	0.000	0.000	0.000	0.000	1.000	-311,589,249.37	356.88	-0.020	0.000
0.800	0.200	0.000	0.114	0.013	0.872	-237,192,151.73	291.89	0.009	0.425
0.800	0.000	0.200	0.019	0.059	0.923	-277,278,023.12	328.27	0.037	0.316
0.600	0.400	0.000	0.232	0.045	0.723	-153,017,901.28	231.75	0.032	0.713
0.600	0.200	0.200	0.119	0.107	0.774	-197,802,133.72	265.80	0.062	0.691
0.600	0.000	0.400	0.031	0.133	0.836	-240,794,967.94	300.73	0.091	0.527
0.400	0.600	0.000	0.337	0.136	0.526	-52,902,109.74	179.52	0.044	0.976
0.400	0.400	0.200	0.208	0.207	0.586	-105,235,158.13	209.82	0.080	0.966
0.400	0.200	0.400	0.115	0.224	0.661	-155,078,238.13	241.36	0.113	0.857
0.400	0.000	0.600	0.036	0.227	0.737	-201,664,918.01	274.51	0.145	0.681
0.200	0.800	0.000	0.449	0.288	0.263	74,340,257.91	140.76	0.039	1.069
0.200	0.600	0.200	0.267	0.414	0.319	10,580,681.67	165.39	0.081	1.082
0.200	0.400	0.400	0.168	0.409	0.423	-51,406,013.14	190.90	0.123	1.030
0.200	0.200	0.600	0.095	0.378	0.527	-107,803,625.97	219.18	0.161	0.928
0.200	0.000	0.800	0.029	0.348	0.623	-159,117,679.50	249.99	0.195	0.764
0.000	1.000	0.000	0.855	0.000	0.145	219,526,333.41	110.91	0.021	0.415
0.000	0.800	0.200	0.416	0.576	0.009	163,344,940.32	139.30	0.059	0.724
0.000	0.600	0.400	0.142	0.713	0.146	48,121,904.03	166.82	0.098	0.799
0.000	0.400	0.600	0.026	0.782	0.192	5,017,561.59	184.40	0.150	0.604
0.000	0.200	0.800	0.031	0.624	0.345	-51,985,177.33	201.25	0.203	0.768
0.000	0.000	1.000	0.000	0.517	0.483	-111,490,937.43	227.99	0.243	0.693
0.333	0.333	0.333	0.166	0.270	0.563	-105,847,119.72	213.06	0.107	0.975
0.667	0.167	0.167	0.102	0.080	0.817	-218,385,863.64	280.17	0.050	0.601
0.167	0.667	0.167	0.297	0.455	0.248	44,834,303.81	156.03	0.072	1.065
0.167	0.167	0.667	0.078	0.402	0.519	-108,378,214.06	220.67	0.175	0.906
0.254	**0.625**	**0.121**	**0.304**	**0.327**	**0.369**	**0.00**	**165.41**	**0.067**	**1.095**

Note: values in bold represent the final solution to the problem.

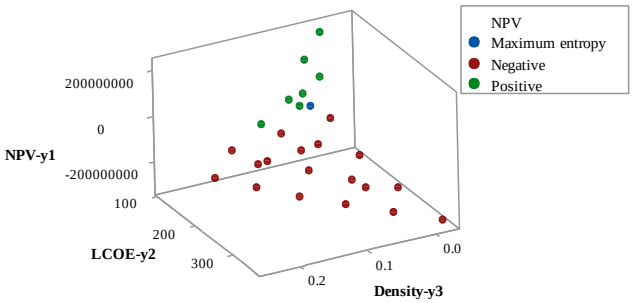

Figure 9 – Pareto Frontier - Scenario 1.

To obtain the final solution for the studied problem, Shannon's entropy metric, as shown in Equation 6, is used. Maximizing the entropy measure allows finding an optimal point with maximum diversification in a system with different components, generating the response with the maximum integration of storage, with the constraint of maintaining the economic viability of the response found ($NPV \geq 0$). Thus, the final solution for Case 1 is obtained as: % Wind (x_1) = 30.4%; % Solar (x_2) = 32.7%; % ESS (x_3) = 36.9%; NPV (y_1) = R$ 0.00; LCOE (y_2) = R$ 165.41; and diversified energy production density (y_3) = 0.067.

4.2. Results for Scenario 2

In Scenario 2, the cost of investment is R$ 8,000,000 per MW installed with payoutfor storage services of R$ 0.00 per MWh. Again, the values of the response variables (y_i), NPV, LCOE and diversified energy production density are calculated for the entire experimental arrangement, as shown in Table 6.

Table 6–Experimental arrangement - Scenario 2

N	Wind (%)	Solar (%)	ESS (%)	NPV (R$)	LCOE (R$/MWh)	$\rho_e \Delta$ (dimensionless)
1	1.000	0.000	0.000	317,834,128.48	108.18	0.000
2	0.750	0.250	0.000	243,949,569.68	119.67	0.032
3	0.750	0,000	0.250	-4,845,647.71	177.77	0.027
4	0.500	0.500	0.000	185,237,478.18	132.05	0.053
5	0.500	0.250	0.250	-63,557,739.21	201.95	0.055
6	0.500	0.000	0.500	-312,352,956.60	289.02	0.035
7	0.250	0.750	0.000	129,139,448.93	148.39	0.059
8	0.250	0.500	0.250	-119,655,768.45	235.22	0.081
9	0.250	0.250	0.500	-368,450,985.84	348.56	0.062
10	0.250	0.000	0.750	-617,246,203.23	502.72	0.024
11	0,000	1.000	0.000	71,347,361.75	173.00	0.000
12	0,000	0.750	0.250	-177,447,855.64	287.85	0.209
13	0,000	0.500	0.500	-426,243,073.03	449.34	0.260
14	0,000	0.250	0.750	-675,038,290.42	693.15	0.151
15	0,00	0.000	1.000	-924,176,451.30	1104.14	0.000
16	0.333	0.333	0.333	-178,236,458.75	250.64	0.069
17	0.667	0.167	0.167	63,936,897.24	161.64	0.041
18	0.167	0.667	0.167	-53,444,548.50	214.28	0.089
19	0.167	0.167	0.667	-551,034,983.28	481.91	0.047

The equations modeled from experimental data can be seen in Table 7.

Table 7–Mathematical models for objective functions - Scenario 2

Terms	NPV (R$)	LCOE (R$/MWh)	$\rho_e \Delta$ (dimensionless)
% Wind	**314,478,175.553**	**138.969**	**0.002**
% Solar	**72,991,327.735**	**178.888**	**0.013**
% ESS	**-922,420,379.236**	**1039.782**	**-0.020**
% Wind x *% Solar*	**-36,299,264.425**	-51.057	**0.209**
% Wind x *% ESS*	**-35,705,084.737**	**-1251.035**	**0.178**
% Solar x *% ESS*	-5,492,401.957	**-637.584**	**0.984**
% Wind x *% Solar* x *% ESS*	**152,269,421.149**	-	**-2.453**
p-value	0.000	0.000	0.000
R^2 (%)	100.00%	98.18%	95.08%
R^2adjusted (%)	99.99%	97.48%	92.61%

Values in bold represent significant terms in the models (p-value < 5%).

The p-values for the objective functions under analysis, obtained from the ANOVA test, show a statistically significant regression at the 5% significance level, proving the adequacy of the functions, and the values of R^2 and R^2 adjusted show that the models have a good fit. Figures 10, 11

and 12 show the response surfaces for NPV (y_1), LCOE (y_2) and diversified energy production density (y_3), respectively.

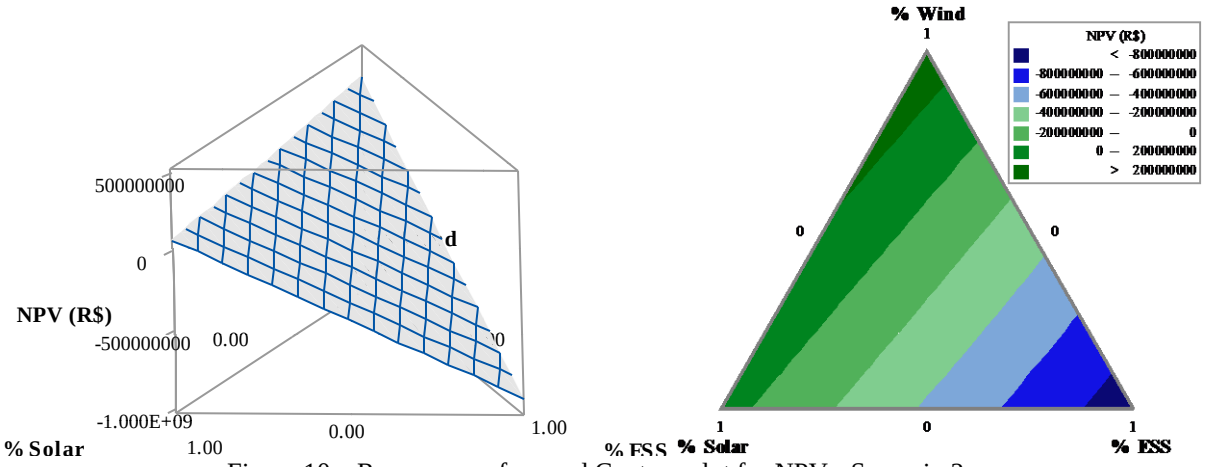

Figure 10 – Response surface and Contour plot for NPV - Scenario 2.

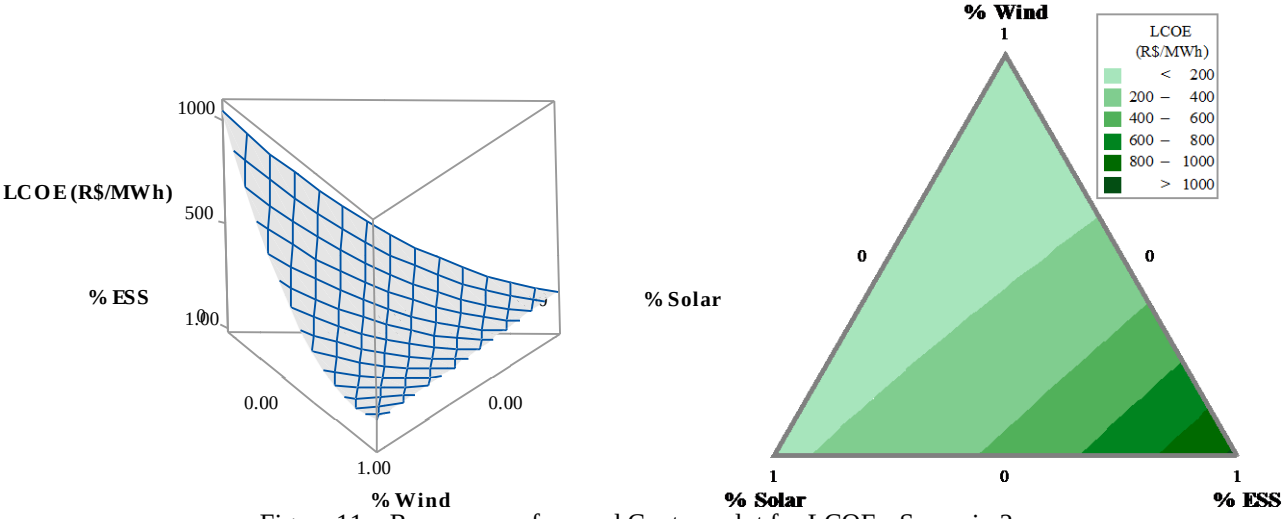

Figure 11 – Response surface and Contour plot for LCOE - Scenario 2.

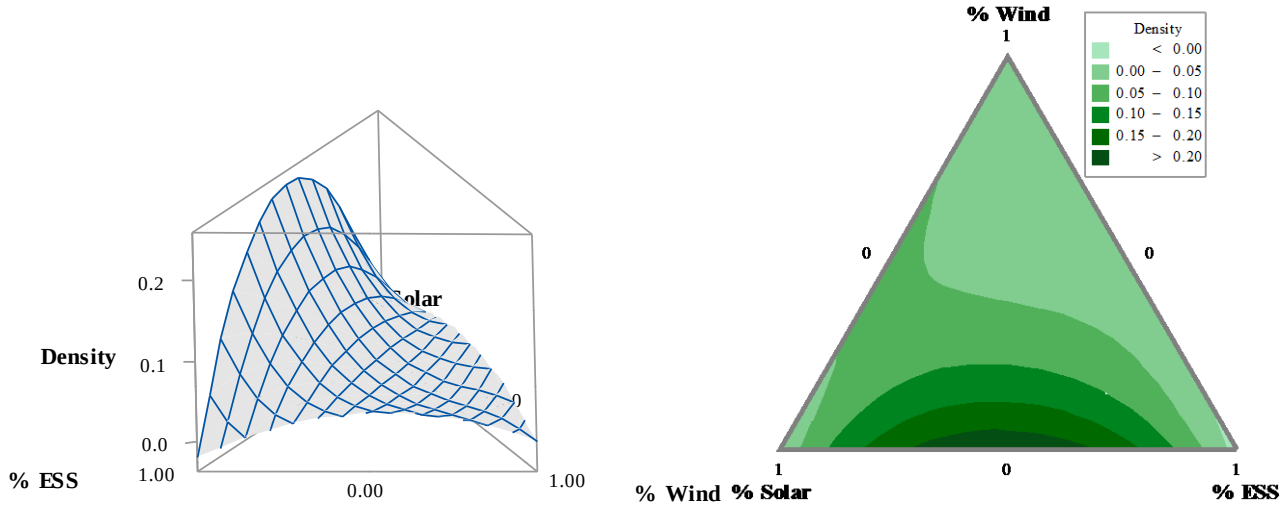

Figure 12 - Response Surface and Contour plot for Diversified Energy Production Density - Scenario 2.

As in Case 1, to implement the NBI optimization process, the payoff matrix is initially estimated, obtaining the results presented in Table 8, which represent the minimum value for NPV, the minimum value for LCOE, and the maximum value for diversified energy production density.

Table 8–Payoff matrix for objective functions - Scenario 2

NPV (R$)	LCOE (R$/MWh)	$\rho_e \Delta$ (dimensionless)
-922,421,301.66	1039.78	-0.020
137,047,667.25	**114.46**	0.021
-409,458,150.69	435.74	**0.243**

Note: values in bold represent individual optimum.

To carry out the multiobjective optimization process, the NBI approach is used, as presented in Equation 5. The results presented in Table 9 constitute the Pareto optimal set for the multiobjective problem. Figure 13 graphically presents the obtained Pareto Frontier.

Table 9 - Pareto Optimal Set - Scenario 2

Weights			% Wind	% Solar	% ESS	NPV (R$)	LCOE	$\rho_e \Delta$	Entropy
w_1	w_2	w_3	(x_1)	(x_2)	(x_3)		(R$/MWh)	(dimensionless)	
1.000	0.000	0.000	0.000	0.000	1.000	-922,421,301.66	1039.78	-0.020	0.000
0.800	0.200	0.000	0.110	0.013	0.877	-777,060,259.34	801.97	0.009	0.415
0.800	0.000	0.200	0.023	0.060	0.917	-835,566,790.31	906.50	0.038	0.334
0.600	0.400	0.000	0.221	0.043	0.736	-611,861,980.29	579.89	0.031	0.694
0.600	0.200	0.200	0.116	0.105	0.779	-677,078,475.40	679.09	0.062	0.681
0.600	0.000	0.400	0.037	0.137	0.826	-742,022,148.00	778.51	0.093	0.551
0.400	0.600	0.000	0.319	0.117	0.564	-415,819,908.11	382.26	0.044	0.939
0.400	0.400	0.200	0.196	0.191	0.613	-492,877,758.73	472.07	0.079	0.935
0.400	0.200	0.400	0.111	0.220	0.670	-568,541,305.68	563.00	0.113	0.845
0.400	0.000	0.600	0.041	0.234	0.726	-640,877,050.90	656.56	0.146	0.703
0.200	0.800	0.000	0.407	0.252	0.341	-171,920,310.68	222.56	0.042	1.080
0.200	0.600	0.200	0.254	0.342	0.404	-270,045,665.26	295.68	0.083	1.081
0.200	0.400	0.400	0.162	0.362	0.476	-363,117,906.65	372.80	0.123	1.016
0.200	0.200	0.600	0.091	0.363	0.546	-449,798,277.90	454.99	0.160	0.917
0.200	0.000	0.800	0.031	0.356	0.613	-530,795,693.78	541.68	0.196	0.776
0.000	1.000	0.000	0.860	0.000	0.140	137,048,390.33	114.46	0.020	0.405
0.000	0.800	0.200	0.289	0.593	0.118	20,444,969.49	172.93	0.067	0.921
0.000	0.600	0.400	0.140	0.651	0.209	-103,743,436.97	225.38	0.116	0.882
0.000	0.400	0.600	0.087	0.603	0.310	-216,440,961.49	286.94	0.162	0.881
0.000	0.200	0.800	0.043	0.556	0.401	-317,423,992.93	357.79	0.204	0.827
0.000	0.000	1.000	0.000	0.517	0.483	-409,458,133.09	435.74	0.243	0.693
0.333	0.333	0.333	0.158	0.253	0.590	-477,893,134.74	466.87	0.106	0.950
0.667	0.167	0.167	0.100	0.080	0.820	-721,804,777.13	736.17	0.050	0.595
0.167	0.667	0.167	0.281	0.368	0.351	-210,795,029.96	258.66	0.076	1.092
0.167	0.167	0.667	0.076	0.389	0.535	-442,985,640.49	451.85	0.174	0.897
0.061	**0.873**	**0.066**	**0.448**	**0.374**	**0.177**	**0.00**	**163.30**	**0.044**	**1.034**

Note: values in bold represent the final solution to the problem.

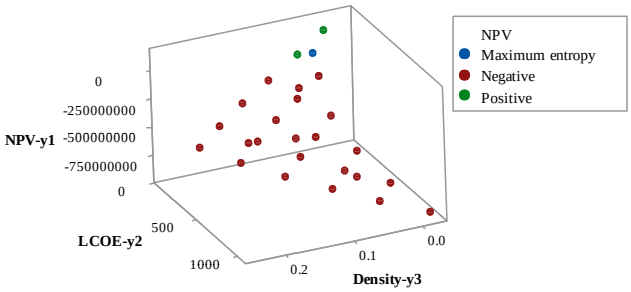

Figure 13 - Pareto Frontier - Scenario 2.

The final solution for Case 2 is obtained as: % Wind (x_1) = 44.8%; % Solar (x_2) = 37.4%; % ESS (x_3) = 17.7%; NPV (y_1) = R$ 0.00; LCOE (y_2) = R$ 163.30; and diversified energy production density (y_3) = 0.044. This result has been achieved by maximizing the entropy measure, since the economic viability of the response found is maintained ($NPV \geq 0$).

4.3. Results for Scenario 3

The experimental data for Scenario 3 (investment of R$ 2,000,000.00 per MW installed with the payout for storage services of R$ 380.12 per MWh) are presented in Table 10, while the mathematical models for NPV (y_1), LCOE (y_2), and diversified energy production density (y_3) are presented in Table 11.

Table 10–Experimental arrangement - Scenario 3

N	Wind (%)	Solar (%)	ESS (%)	NPV (R$)	LCOE (R$/MWh)	$\rho_e \Delta$ (dimensionless)
1	1.000	0.000	0.000	317,834,128.48	108.18	0.000
2	0.750	0.250	0.000	243,949,569.68	119.67	0.032
3	0.750	0,000	0.250	222,670,504.23	129.87	0.027
4	0.500	0.500	0.000	185,237,478.18	132.05	0.053
5	0.500	0.250	0.250	163,958,412.73	145.44	0.055
6	0.500	0.000	0.500	142,679,347.27	162.12	0.035
7	0.250	0.750	0.000	129,139,448.93	148.39	0.059
8	0.250	0.500	0.250	107,860,383.48	166.77	0.081
9	0.250	0.250	0.500	86,581,318.03	190.77	0.062
10	0.250	0.000	0.750	65,302,252.58	223.40	0.024
11	0,000	1.000	0.000	71,347,361.75	173.00	0.000
12	0,000	0.750	0.250	50,068,296.30	200.59	0.209
13	0,000	0.500	0.500	28,789,230.85	239.38	0.260
14	0,000	0.250	0.750	7,510,165.40	297.95	0.151
15	0,00	0.000	1.000	-13,768,900.05	396.57	0.000
16	0.333	0.333	0.333	125,118,410.50	162.97	0.069
17	0.667	0.167	0.167	215,614,331.86	129.38	0.041
18	0.167	0.667	0.167	98,232,886.12	167.67	0.089
19	0.167	0.167	0.667	55,674,755.22	226.30	0.047

Table 11– Mathematical models for objective functions - Scenario 3

Terms	NPV (R$)	LCOE (R$/MWh)	$\rho_e \Delta$ (dimensionless)
% Wind	**314,508,332.410**	**118.717**	**0.002**
% Solar	**73,021,484.592**	**174.244**	**0.013**
% ESS	**-12,094,777.214**	**379.197**	**-0.020**
% Wind x *% Solar*	**-36,411,869.284**	-46.873	**0.209**
% Wind x *% ESS*	**-36,411,869.284**	**-366.450**	**0.178**
% Solar x *% ESS*	-6,199,186.505	**-153.840**	**0.984**
% Wind x *% Solar* x *% ESS*	**153,825,154.528**	-	**-2.453**
p-value	0.000	0.000	0.000
R^2 (%)	99.93%	98.14%	95.08%
R^2adjusted (%)	99.90%	97.42%	92.61%

Values in bold represent significant terms in the models (p-value < 5%).

The mathematical models show both adequacy (p-values< 5%) and good fit (R^2 adjusted > 90%). Figures 14, 15 and 16 show the response surfaces for NPV (y_1), LCOE (y_2) and diversified energy production density (y_3), respectively.

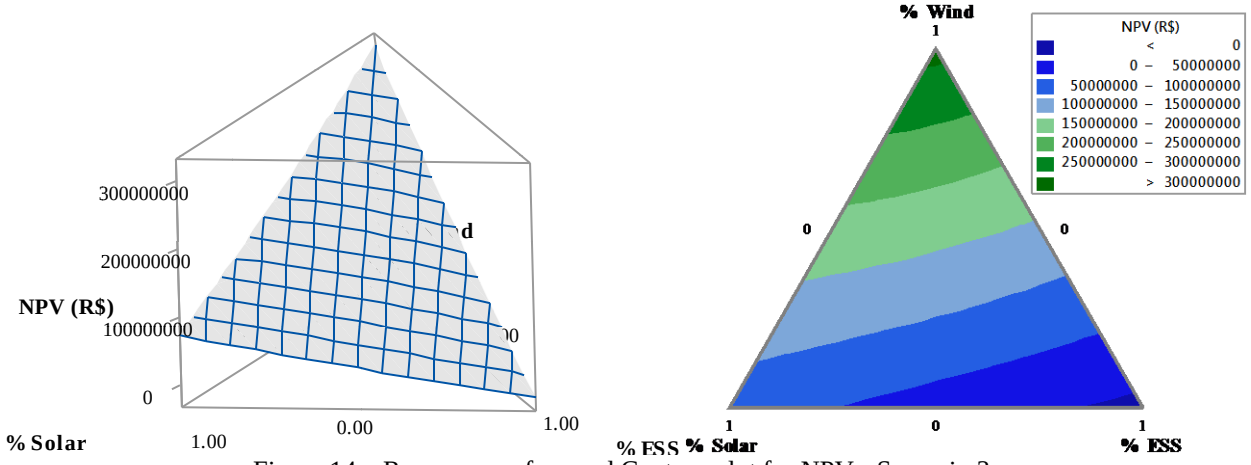

Figure 14 – Response surface and Contour plot for NPV - Scenario 3.

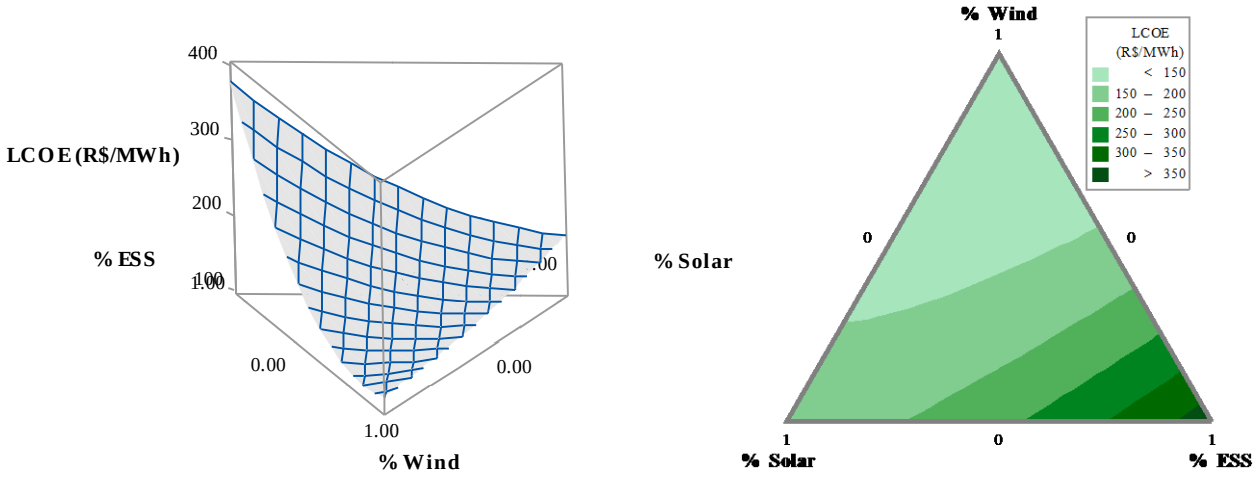

Figure 15 – Response surface and Contour plot for LCOE - Scenario 3.

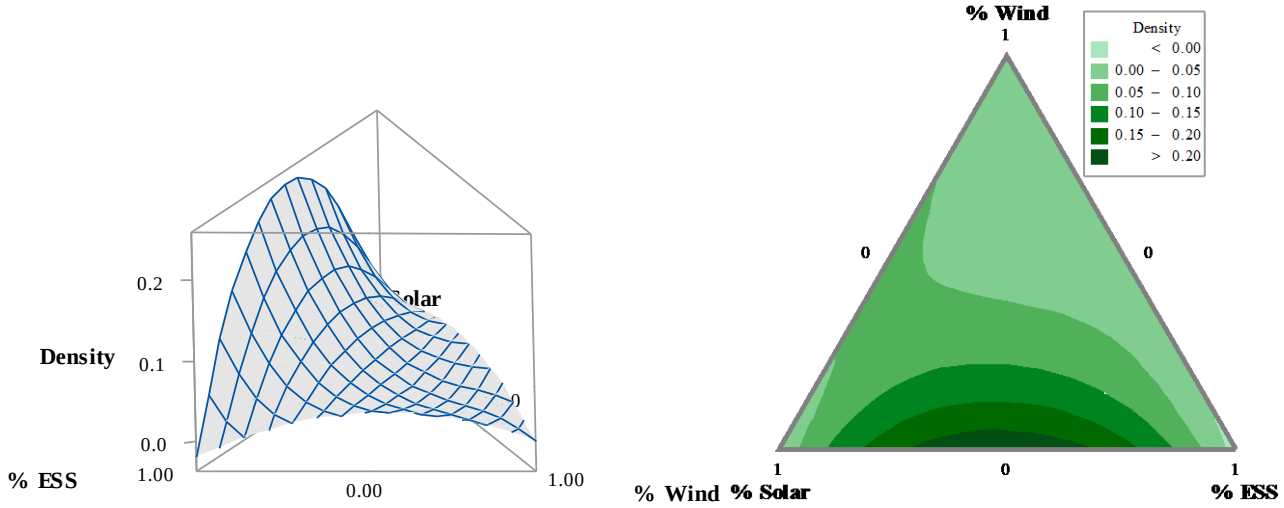

Figure 16 - Response Surface and Contour plot for Diversified Energy Production Density - Scenario 3.

Table 12 presents the data from the payoff matrix, which represents the individual optimal of the problem response variables, i.e., NPV, LCOE, and diversified energy production density.

Table 12–Payoff matrix for objective functions - Scenario 3

NPV (R$)	**LCOE (R$/MWh)**	$\rho_e \Delta$ **(dimensionless)**
-12,094,789.31	379.20	-0.020
262,781,569.49	**111.06**	0.021
30,337,131.41	234.88	**0.243**

Note: values in bold represent individual optimum.

The results presented in Table 13 constitute the Pareto optimal set for the multiobjective problem obtained by the NBI approach, which is graphically presented in Figure 17.

Table 13–Pareto Optimal Set - Scenario 3

Weights			***% Wind***	***% Solar***	***% ESS***	NPV (R$)	LCOE	$\rho_e \Delta$	Entropy
w_1	w_2	w_3	(x_1)	(x_2)	(x_3)		(R$/MWh)	(dimensionless)	
1.000	0.000	0.000	0.000	0.000	1.000	-12,094,789.31	379.20	-0.020	0.000
0.800	0.200	0.000	0.118	0.023	0.859	24,899,167.45	303.36	0.016	0.470
0.800	0.000	0.200	0.016	0.053	0.931	-3,086,872.86	350.98	0.032	0.289
0.600	0.400	0.000	0.233	0.086	0.682	66,376,479.54	233.05	0.045	0.811
0.600	0.200	0.200	0.121	0.116	0.763	34,503,141.76	275.87	0.067	0.711
0.600	0.000	0.400	0.028	0.120	0.852	5,969,469.85	322.82	0.084	0.490
0.400	0.600	0.000	0.307	0.322	0.372	112,593,863.28	168.61	0.066	1.095
0.400	0.400	0.200	0.202	0.284	0.514	75,735,883.58	205.27	0.096	1.022
0.400	0.200	0.400	0.115	0.239	0.646	43,837,172.17	248.06	0.118	0.873
0.400	0.000	0.600	0.033	0.207	0.760	14,944,720.13	294.56	0.135	0.647
0.200	0.800	0.000	0.502	0.445	0.052	182,452,111.70	133.36	0.052	0.861
0.200	0.600	0.200	0.233	0.542	0.225	107,214,038.56	163.56	0.089	1.007
0.200	0.400	0.400	0.121	0.596	0.283	76,413,527.04	183.59	0.139	0.921
0.200	0.200	0.600	0.088	0.431	0.481	51,943,771.43	218.73	0.171	0.929
0.200	0.000	0.800	0.029	0.323	0.648	23,533,696.11	265.82	0.188	0.749
0.000	1.000	0.000	0.851	0.024	0.124	263,734,954.29	112.23	0.019	0.487
0.000	0.800	0.200	0.607	0.393	0.000	211,042,185.32	129.33	0.056	0.670
0.000	0.600	0.400	0.537	0.463	0.000	193,659,203.39	132.77	0.059	0.690
0.000	0.400	0.600	0.100	0.609	0.291	70,706,376.45	187.59	0.151	0.891
0.000	0.200	0.800	0.017	0.662	0.321	48,353,978.33	203.95	0.206	0.706
0.000	0.000	1.000	0.000	0.517	0.483	30,337,119.87	234.88	0.243	0.693
0.333	0.333	0.333	0.160	0.342	0.498	67,541,277.23	209.43	0.121	1.007
0.667	0.167	0.167	0.104	0.086	0.811	26,389,645.87	292.67	0.053	0.616
0.167	0.667	0.167	0.274	0.532	0.193	119,275,681.44	156.52	0.076	1.008
0.167	0.167	0.667	0.072	0.449	0.479	48,194,471.30	221.23	0.183	0.901
0.732	**0.000**	**0.268**	**0.021**	**0.074**	**0.905**	**0.00**	**341.38**	**0.050**	**0.363**

Note: values in bold represent the final solution to the problem.

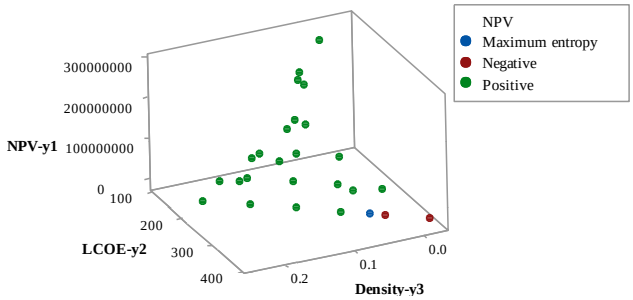

Figure 17 - Pareto Frontier - Scenario 3.

The blue point in Figure 17 is the final solution for the problem, representing the maximum integration of storage, with the restriction of the maintenance of the economic viability. The final solution for Case 3 is obtained as: % Wind (x_1) = 2.1%; % Solar (x_2) = 7.4%; % ESS (x_3) = 90.5%; NPV (y_1) = R$ 0.00; LCOE (y_2) = R$ 341.38; and diversified energy production density (y_3) = 0.050.

4.4. Results for Scenario 4

Finally, based on the initial conditions stipulated in relation to the ESS for Scenario 4 (investment of R$ 8,000,000.00 per MW installed with payout for storage services of R$ 380.12 per MWh), the values of the response variables (y_i) NPV, LCOE and diversified energy production density are calculated, for the entire experimental arrangement, as shown in Table 14.

Table 14–Experimental arrangement - Scenario 4

N	Wind (%)	Solar (%)	ESS (%)	NPV (R$)	LCOE (R$/MWh)	$\rho_e \Delta$ (dimensionless)
1	1.000	0.000	0.000	317,834,128.48	108.18	0.000
2	0.750	0.250	0.000	243,949,569.68	119.67	0.032
3	0.750	0,000	0.250	69,628,880.71	179.41	0.027
4	0.500	0.500	0.000	185,237,478.18	132.05	0.053
5	0.500	0.250	0.250	10,916,789.21	203.89	0.055
6	0.500	0.000	0.500	-163,403,899.77	293.37	0.035
7	0.250	0.750	0.000	129,139,448.93	148.39	0.059
8	0.250	0.500	0.250	-45,181,240.04	237.57	0.081
9	0.250	0.250	0.500	-219,501,929.01	353.96	0.062
10	0.250	0.000	0.750	-393,822,617.98	512.29	0.024
11	0,000	1.000	0.000	71,347,361.75	173.00	0.000
12	0,000	0.750	0.250	-102,973,327.22	290.84	0.209
13	0,000	0.500	0.500	-277,294,016.19	456.53	0.260
14	0,000	0.250	0.750	-451,614,705.16	706.68	0.151
15	0,00	0.000	1.000	-625,935,394.13	1127.94	0.000
16	0.333	0.333	0.333	-78,937,087.53	253.64	0.069
17	0.667	0.167	0.167	113,586,582.85	162.74	0.041
18	0.167	0.667	0.167	-3,794,862.89	215.88	0.089
19	0.167	0.167	0.667	-352,436,240.83	490.66	0.047

The data presented in Table 14 are used to generate the equations for NPV (y_1), LCOE (y_2) and diversified energy production density (y_3) as a function of the proportions of each technology considered (x_i). The equations obtained can be seen in Table 15.

Table 15–Mathematical models for objective functions - Scenario 4

Terms	NPV (R$)	LCOE (R$/MWh)	$\rho_e \Delta$ (dimensionless)
% Wind	**314,508,332.410**	**139.642**	**0.002**
% Solar	**73,021,484.592**	**179.027**	**0.013**
% ESS	**-624,261,271.294**	**1062.095**	**-0.020**
% Wind x *% Solar*	**-36,411,869.284**	-51.235	**0.209**
% Wind x *% ESS*	**-36,411,869.284**	**-1280.624**	**0.178**
% Solar x *% ESS*	-6,199,186.505	**-653.449**	**0.984**
% Wind x *% Solar* x *% ESS*	**153,825,154.528**		**-2.453**
p-value	0.000	0.000	0.000
R^2 (%)	99.99%	98.19%	95.08%
R^2adjusted (%)	99.99%	97.49%	92.61%

Values in bold represent significant terms in the models (p-value < 5%).

One more time, the adequacy of the models is analyzed by ANOVA. The p-values for the objective functions under analysis show a statistically significant regression at the 5% significance level, proving the adequacy of the functions. Also, the values of R^2 and R^2 adjusted show that the models have a good fit. Figures 18, 19 and 20 show the response surfaces for NPV (y_1), LCOE (y_2) and diversified energy production density (y_3), respectively.

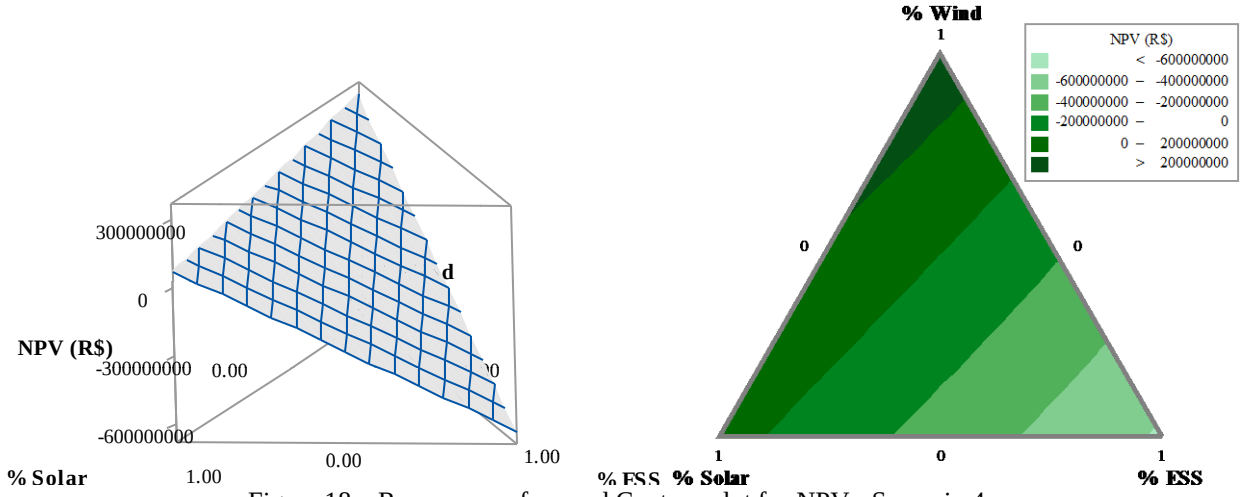

Figure 18 – Response surface and Contour plot for NPV - Scenario 4.

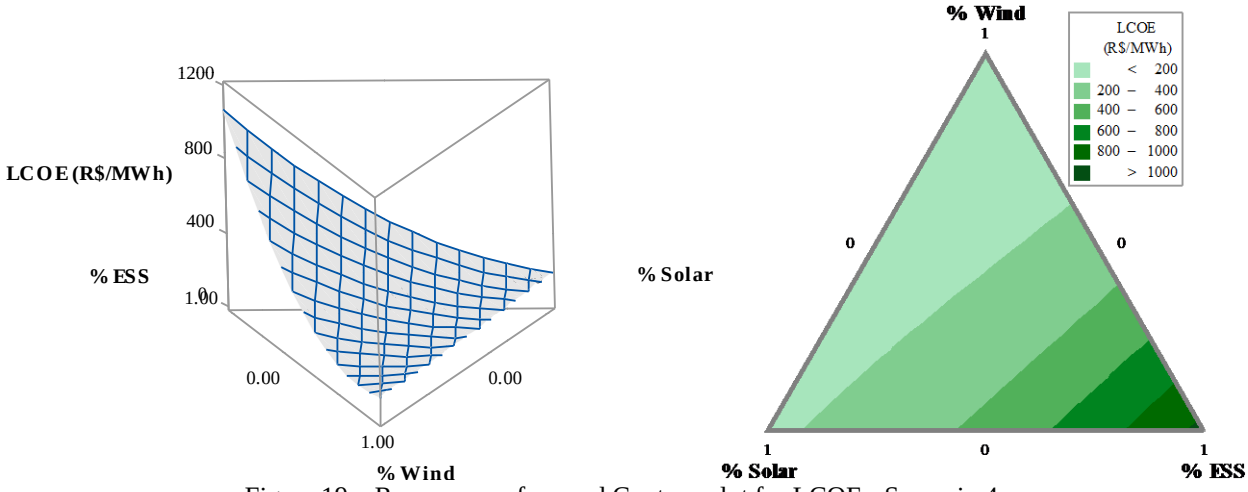

Figure 19 – Response surface and Contour plot for LCOE - Scenario 4.

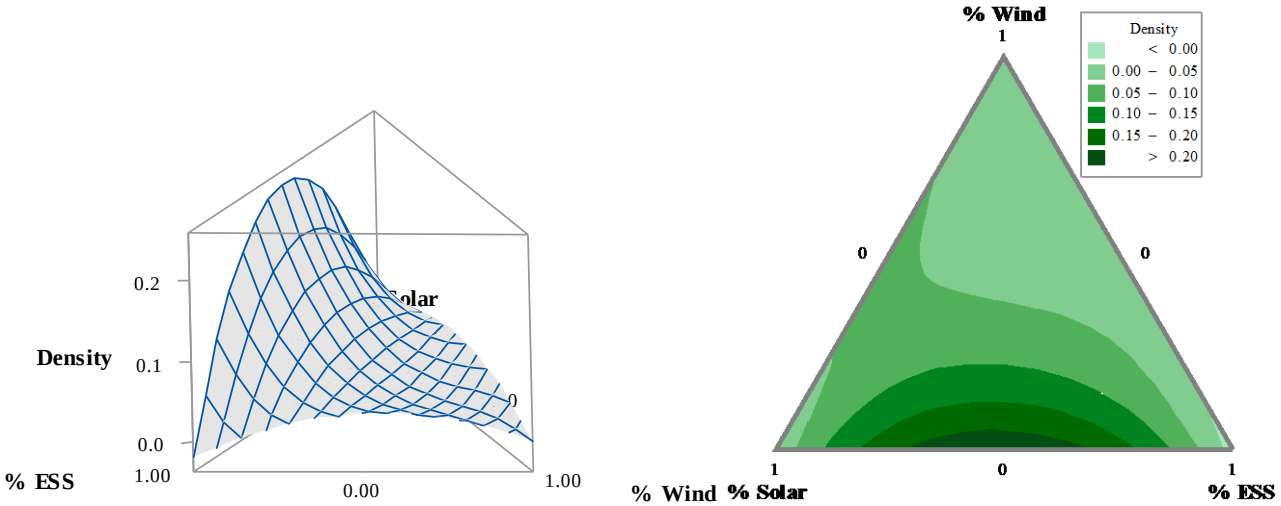

Figure 20 - Response Surface and Contour plot for Diversified Energy Production Density - Scenario 4.

Another time, as in the cases presented above, to implement the NBI optimization process, the payoff matrix is initially estimated, obtaining the results presented in Table 16. In order to define the configuration of a hybrid plant that would allow the inclusion of the ESS while maintaining the project's feasibility, that is, with a NPV greater than or equal to zero (0), NPV has been minimized, LCOE has been minimized too, and the diversified energy production density response ($\rho_e \Delta$) has been maximized.

Table 16–Payoff matrix for objective functions - Scenario 4

NPV (R$)	LCOE (R$/MWh)	$\rho_e \Delta$ (dimensionless)
-624,261,895.56	1062.10	-0.020
178,848,584.13	**114.60**	0.020
-265,520,134.63	442.63	**0.243**

Note: values in bold represent individual optimum.

To carry out the multiobjective optimization process, the NBI approach is used, as presented in Equation 5. The results presented in Table 17 constitute the Pareto optimal set for the multiobjective problem. Figure 21 graphically presents the obtained Pareto frontier.

Table 17–Pareto Optimal Set - Scenario 4

Weights			*% Wind*	*% Solar*	*% ESS*	NPV (R$)	LCOE	$\rho_e \Delta$	Entropy
w_1	w_2	w_3	(x_1)	(x_2)	(x_3)		(R$/MWh)	(dimensionless)	
1.000	0.000	0.000	0.000	0.000	1.000	-624,261,271.29	1062.09	-0.020	0.000
0.800	0.200	0.000	0.110	0.014	0.876	-514,586,419.99	816.67	0.010	0.420
0.800	0.000	0.200	0.023	0.059	0.918	-562,778,658.82	926.93	0.037	0.331
0.600	0.400	0.000	0.220	0.047	0.733	-389,991,349.70	587.61	0.033	0.704
0.600	0.200	0.200	0.116	0.106	0.778	-444,168,847.26	691.31	0.063	0.683
0.600	0.000	0.400	0.037	0.135	0.828	-496,913,722.04	796.58	0.092	0.548
0.400	0.600	0.000	0.315	0.130	0.555	-242,665,272.83	383.52	0.046	0.956
0.400	0.400	0.200	0.195	0.196	0.608	-306,807,449.98	476.27	0.080	0.941
0.400	0.200	0.400	0.111	0.221	0.668	-368,116,039.87	572.14	0.113	0.847
0.400	0.000	0.600	0.041	0.232	0.728	-426,082,591.44	671.68	0.145	0.700
0.200	0.800	0.000	0.399	0.279	0.322	-59,303,752.40	218.98	0.045	1.088
0.200	0.600	0.200	0.249	0.361	0.390	-140,930,742.12	292.54	0.086	1.081
0.200	0.400	0.400	0.159	0.373	0.468	-216,158,590.77	373.13	0.125	1.016

0.200	0.200	0.600	0.091	0.366	0.543	-285,306,993.78	460.39	0.161	0.917
0.200	0.000	0.800	0.032	0.354	0.615	-349,428,989.14	553.17	0.195	0.776
0.000	1.000	0.000	0.860	0.000	0.140	178,849,069.28	114.60	0.020	0.405
0.000	0.800	0.200	0.229	0.691	0.080	67,647,772.91	172.99	0.068	0.795
0.000	0.600	0.400	0.075	0.764	0.161	-22,932,035.82	219.43	0.119	0.694
0.000	0.400	0.600	0.074	0.635	0.292	-113,947,322.13	282.68	0.165	0.840
0.000	0.200	0.800	0.039	0.567	0.394	-193,546,178.86	358.47	0.205	0.815
0.000	0.000	1.000	0.000	0.517	0.483	-265,520,129.81	442.63	0.243	0.693
0.333	0.333	0.333	0.157	0.258	0.585	-299,285,848.80	471.37	0.107	0.954
0.667	0.167	0.167	0.100	0.080	0.819	-476,861,199.50	750.17	0.050	0.596
0.167	0.667	0.167	0.274	0.393	0.333	-95,447,349.09	254.31	0.079	1.088
0.167	0.167	0.667	0.075	0.392	0.533	-281,941,320.73	457.51	0.175	0.897
0.131	**0.833**	**0.036**	**0.406**	**0.355**	**0.239**	**0.00**	**187.21**	**0.047**	**1.076**

Note: values in bold represent the final solution to the problem.

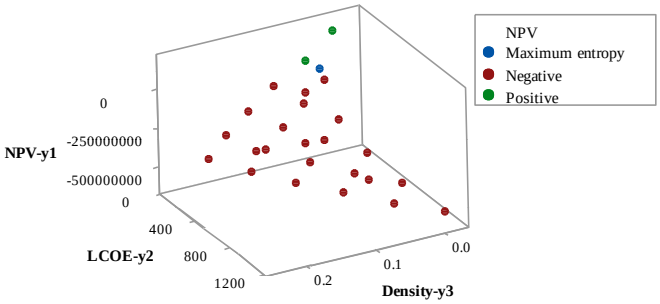

Figure 21 - Pareto Frontier - Scenario 4.

The final solution for Case 4 is obtained as: % Wind (x_1) = 40.6%; % Solar (x_2) = 35.5%; % ESS (x_3) = 23.9%; NPV (y_1) = R$ 0.00; LCOE (y_2) = R$ 187.21; and diversified energy production density (y_3) = 0.047.

4.5. Comparison between scenarios

In order to compare the results found for the different analyzed scenarios, Table 18 is constructed. Figure 22, on the other hand, presents the Pareto frontiers for the four scenarios.

Table 18–Consolidated Results

Scenarios	***Cost of investment in ESS (R$/MW)***	***Payout for ESS services (R$/MWh)***	**NPV (R$)**	**LCOE (R$/MWh)**	$\rho_e \Delta$ **(dimensionless)**	***% Wind*** (x_1)	***% Solar*** (x_2)	***% ESS*** (x_3)
1	2,000,000.00	0.00	0.00	165.41	0.067	0.304	0.327	0.369
2	8,000,000.00	0.00	0.00	163.30	0.044	0.448	0.374	0.177
3	2,000,000.00	380.12	0.00	341.38	0.050	0.021	0.074	0.905
4	8,000,000.00	380.12	0.00	187.21	0.047	0.406	0.355	0.239

In Scenario 3, which presents a lower investment cost and a significant payout for the service provided by the ESS, it is possible to implement an autonomous storage system designed only for this purpose. That is, without being combined with a power generation plant. In Scenario 2, it would only be possible to implement 17.7% of the 60 MW installed capacity in the ESS. However, it should be noted that the sale prices of wind and solar energy considered in this study are the auction ceiling prices, and in this situation, as we would already be at the limit of the project viability, it would not be possible to implement any discount on the price of energy. This means that such a project would only be possible with an energy price subsidy mechanism that would offset the economic deficit caused by the ESS.

In general, the LCOE can be considered as the minimum price for the project feasibility. The results suggest that the greater the participation of the ESS, the greater the LCOE of the project, hence

the greater the need for payout so that the integration of the ESS can be made viable. In this sense, the LCOE obtained in the optimization can serve as a reference for the status of the technology compared to traditional projects, without the integration of ESS. In this study, wind power generation is more competitive than solar photovoltaic generation (LCOE of R$108.18/MWh for wind and R$173.00/MWh for solar), which is in line with the most recent worldwide technical studies [96,97].Thus, when analyzing the LCOE for the configuration of hybrid plants with utility-scale ESS, it presents itself as a competitive option for all scenarios, despite the economic deficit caused by the integration of the utility-scale ESS. It is important to highlight that Scenario 3, which presents the highest LCOE, is the scenario that considers the best conditions for the integration of utility-scale ESS (lower investment cost and maximum payout) and, therefore, allows for greater participation of this type of technology.

While the diversified energy production density ($\rho_e \Delta$) has shown itself very useful, allowing the integration of ESS in the solution space of the formulated problem, it does not have a physical meaning. Thus, the total energy production (Equation 8), the occupied area, and the energy production density (Equation 7) have been calculated for the hybrid plant configurations achieved in each scenario. Scenario 1 obtained the following results: 1,772,617 MWh of total energy production; 8,436,271 m^2 of the area; and 0.2101 MWh/m^2 of energy production density. For Scenario 2, the following results are achieved: 2,470,848 MWh of total energy production; 12,249,496 m^2 of the area; and 0.2017 MWh/m^2 of energy production density. The results of total energy production, occupied area, and energy production density for Scenario 3 are, respectively, 52,988 MWh, 665,150 m^2, and 0.0797 MWh/m^2. Finally, for Scenario 4, the results are 2,252,350 MWh, 11,111,351 m^2, and 0.2027 MWh/m^2 for total energy production, occupied area, and energy production density, respectively. Scenarios 2 and 4, which have the greatest share of wind energy, have the highest total energy production and the largest occupied areas. This is expected as this technology has a higher capacity factor and greater area demand for its installation. What is noteworthy is that the production metric relative to the occupied area did not vary much between the scenarios, with the most diversified scenario (Scenario 1), performing better in this metric. The exception is Scenario 3, with a high share of ESS, which has the worst performance in terms of both total production and production density.

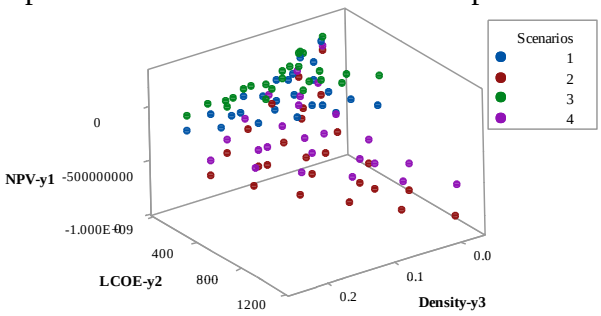

Figure 22 – Pareto frontiers for all studied scenarios.

Based on Figure 22, it is noticed that, in Scenarios 2 and 4, in which an ESS investment cost of R$ 8,000,000.00 is used, the points are more dispersed in the Pareto-optimal frontier with most NPV values below zero, indicating economically unfeasible solutions. From this it appears that the cost of investment in ESS, in the range used, has a greater impact on the viability of the energy generation project with ESS than the payout for the service provided. Figure 23 shows a comparison of the Pareto frontiers for Scenarios 1 (investment of R$ 2,000,000.00 per MW installed with payout for storage services of R$ 0.00 per MWh) and 4 (investment of R$ 8,000,000.00 per MW installed with payout for storage services of R$ 380.12 per MWh).

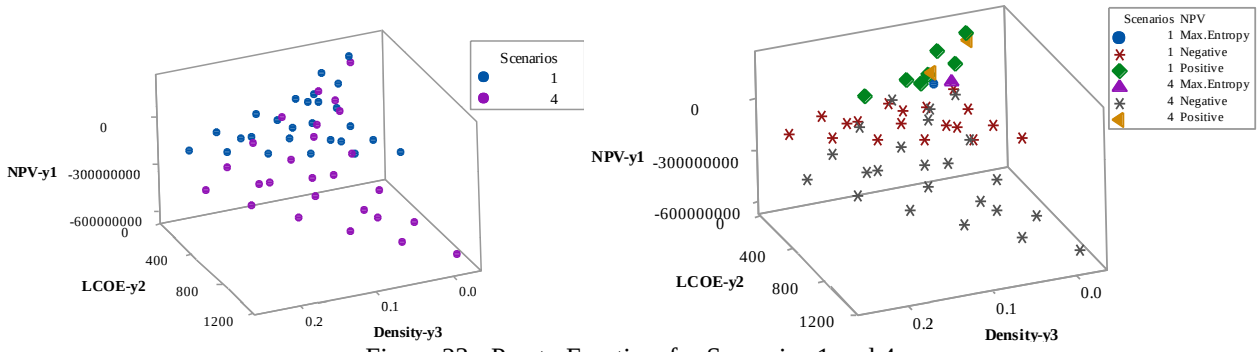

Figure 23 - Pareto Frontiers for Scenarios 1 and 4.

Comparing Scenarios 1 and 4 shown in Figure 23, Scenario 1 has more Pareto-optimal points in the feasibility area, which generates greater flexibility for a possible composition of the hybrid wind-photovoltaic plant with utility-scale Li-ion battery ESS. In addition, although the final solution to the problem is very close in both scenarios, which is understandable by the restrictions adopted (maximum entropy and $NPV = 0$), Scenario 1 would allow the use of a higher proportion of ESS in the project: 36.9% against 23.9% in Scenario 4.

4.6. Policy implications

As shown, the integration of a utility-scale battery ESS in hybrid wind-photovoltaic projects should still go a long way before it can present itself as an economically viable option. In the current scenario, the investment costs are still high and payout for the various services provided to the grid is not properly defined due to the absence of relevant regulation. Hence, the possibility of integration of storage is minimal, reaching only 17.7% of the project capacity, even considering the price paid for the energy generated as the auction ceiling price without considering any discount in the tariff.

Regarding the payout mechanisms of ESS, a regulatory framework that recognizes the value of storage for the electricity system must be sought, creating a mechanism based on maximizing benefits rather than minimizing costs, so that all benefits provided by the ESS can be recognized and compensated. The regulatory framework must predict whether there will be a defined minimum payment for the services provided, such as the feed-in tariff policies adopted to encourage the generation of energy by RES, and/or whether there will be a subsidized credit line for investments in ESS technology. Another point that needs definition is the contracting modality to be adopted in the storage market. Currently, the main form of contracting energy in Brazil is through auctions in the Regulated Market, using the lowest tariff criterion. However, Pérez-Arriaga and Knittel [98] and Vivero-Serrano et al. [99] reinforce that conventional bidding structures may have to be revised to reflect resources' operational constraints. In addition, the creation of the electricity storage agent figure would allow for the generation of multiple revenues, avoid double taxation of storage activity, and allow the creation of clear rules for broad competition in the storage market.

Greater temporal granularity of spot prices associated with unrestricted access to the Free Market may enable the creation of an energy stock exchange in Brazil. In this sense, utility-scale ESS can be implemented to work with price arbitrage. In addition to price arbitrage, in order to generate multiple revenues for utility-scale ESS, it is necessary to create a capacity market, which can be met with the implementation of the proposed separation between ballast and energy in the Brazilian market. Also, it is necessary to reassess the way in which ancillary services are provided and how they are paid. In the current context, it would be possible to create a market for ancillary services, with rapid response services and rapid ramp services, which could be specifically served by more modern technologies, such as lithium-ion batteries. Regardless of the technology, utility-scale ESS could become viable for scenarios where the electricity matrix has a high share of generation from intermittent RES.

In the present study, it is clearly demonstrated that the investment cost has a fundamental impact on the economic viability of hybrid wind-photovoltaic projects with utility-scale battery ESS. In this context, a neglected point in the emerging literature on storage in Brazil and that could be the object of discussions about regulatory adjustments would be industrial policies for the development of the productive chain involving energy storage. In the specific case of Li-ion batteries, Brazil has large reserves of lithium, and the first reserves are found during World War II [100]. In this sense, industrial policies that favor the production chain as a whole, from mining to the final production of batteries, could reduce the cost of the final product, enabling its implementation in the most diverse applications, from batteries for electric vehicles to utility-scale battery ESS. Another possibility would be the creation of tax incentives for the import of equipment, aiming at lowering its cost.

Finally, it is worth noting that since the ESS have a negative total energy balance, integration of ESS implies an increase in the load for the system as a whole and this needs to be considered when preparing long-term planning aiming at the creation of an electricity storage market in Brazil.

5. Conclusion

The present study sought to optimize the configuration of hybrid wind-photovoltaic power plant projects with utility-scale battery ESS and to discuss the application possibilities for regulatory adequacy in Brazil. The proposed study becomes very timely in the context of discussions on the regulatory adjustments necessary for the integration of ESS in the NIS, providing essential information on the economic feasibility of applying this technology in wind-photovoltaic power plant projects already under development in the Brazil. The innovative character of the article focuses on an optimization routine that, by considering different scenarios, contributes to the regulatory advances necessary to promote the technical and economic feasibility of using energy storage in Brazil.

The mixture arrangement design proved to be adequate in order to model the mathematical responses and the NBI optimization methodology found to be efficient in building Pareto frontiers for the scenarios studied. Two financial indicators (NPV and LCOE) and an indicator that relates energy production to the area occupied in its generation were optimized, seeking maximum diversification (diversified energy production density). For each scenario, using Shannon's entropy, the optimal solution was obtained from the most diversified configuration among the economically viable ones. The optimization routine proposed in this study proved to be quite applicable, both due to its ease of implementation and the reduced computational cost, allowing the generation of the Pareto frontier in more complex problems involving three responses (objective functions).

The results show that the investment cost can have a greater impact than the remuneration itself for the services provided. This fact demonstrates that public policies for achieving technical-economic feasibility in the use of utility-scale battery ESS should focus on subsidized lines of credit and/or reduction of import fees in order to reduce the cost of investment. The results also show that appropriate public policies (especially investment cost reduction and a financial compensation system) can even enable projects exclusively dedicated to energy storage.

For future studies, it is suggested to consider the application of the proposed routine in other countries or regions, to use the combination of different energy storage and generation technologies, and to use the routine proposed in countries that already have their regulatory framework in an advanced stage of development to define the optimal mix of projects to be installed, given the previously established market conditions.

Conflicts of Interest: The authors declare that there are no conflicts of interest regarding the publication of this paper.

Acknowledgments: The authors would like to thank the Brazilian National Council for Scientific and Technological Development - CNPq Brazil (Processes 406769/2018-4, 308021/2019-3, 302751/2020-3), the National School of Public Administration - ENAP Brazil (Process 04600.003102/2020-21) and the Coordination for the Improvement of Higher Education Personnel - Capes Brazilfor the financial support and research incentive.

Appendix A. Climatic data

Table A1 –Irradiation data (Wh/m^2) from Caetité-BA

Hour	Irradiation (Wh/m^2)											
	Jan	Feb	Mar	Apr	May	Jun	Jul	Aug	Sep	Oct	Nov	Dec
0 - 1	0	0	0	0	0	0	0	0	0	0	0	0
1 - 2	0	0	0	0	0	0	0	0	0	0	0	0
2 - 3	0	0	0	0	0	0	0	0	0	0	0	0
3 - 4	0	0	0	0	0	0	0	0	0	0	0	0
4 - 5	0	0	0	0	0	0	0	0	0	0	0	0
5 - 6	12	0	0	0	0	0	0	0	0	49	53	47
6 - 7	188	160	129	129	114	91	88	146	177	261	219	216
7 - 8	345	333	301	289	302	299	323	392	371	434	355	355
8 - 9	504	479	432	419	420	430	452	545	549	579	490	493
9 - 10	603	569	536	519	533	538	574	679	676	658	545	572
10 - 11	620	601	569	569	612	617	667	744	740	688	535	570
11 - 12	575	588	556	579	614	643	704	761	747	678	502	549
12 - 13	544	559	538	573	593	643	709	761	740	646	476	517
13 - 14	519	547	525	549	573	622	691	733	702	587	433	485
14 - 15	500	525	507	527	546	596	663	693	649	541	393	449
15 - 16	470	490	476	502	513	556	613	634	575	486	353	413
16 - 17	419	433	428	431	397	430	506	530	463	402	319	369
17 - 18	299	312	217	128	45	45	134	157	132	120	136	247
18 - 19	17	17	0	0	0	0	0	0	0	0	0	0
19 - 20	0	0	0	0	0	0	0	0	0	0	0	0
20 - 21	0	0	0	0	0	0	0	0	0	0	0	0
21 - 22	0	0	0	0	0	0	0	0	0	0	0	0
22 - 23	0	0	0	0	0	0	0	0	0	0	0	0
23 - 24	0	0	0	0	0	0	0	0	0	0	0	0

Source: SWERA [75].

Table A2 –Maximum average temperature (ºC) from Caetité-BA

Month	Maximum average temperature (ºC)
Jan	30
Feb	31
Mar	30
Apr	29
May	25
Jun	25
Jul	25
Aug	26
Sep	29
Oct	31
Nov	32
Dec	32

Source: INPE [76].

Table A3 –Wind speed data (m/s) at 100 m height from Caetité-BA

Hour	Wind Speed (m/s)											
	Jan	Feb	Mar	Apr	May	Jun	Jul	Aug	Sep	Oct	Nov	Dec
0 - 1	9.4	10.3	8.8	10.4	11.5	11.8	13.1	12.9	12.8	12.8	10.3	8.6
1 - 2	9.9	10.9	9.4	11	12.1	12.4	13.6	13.4	13.4	13.1	10.7	8.9
2 - 3	10.4	11.3	9.7	11.5	12.4	12.7	13.9	13.6	13.7	13.3	10.8	9.1
3 - 4	10.8	11.5	9.8	11.7	12.6	12.7	14.1	13.6	13.9	13.2	10.7	9.3
4 - 5	11.1	11.6	10.1	11.8	12.7	12.8	14.1	13.7	14	13.1	10.7	9.5
5 - 6	11.1	11.7	10.2	11.8	12.8	12.8	14.1	13.8	14	13	10.6	9.6
6 - 7	11	11.6	10.2	11.8	12.9	12.8	14.1	13.8	13.9	13	10.6	9.6
7 - 8	10.9	11.4	10.1	11.7	12.9	12.8	14.1	13.7	13.8	12.9	10.6	9.6
8 - 9	10.9	11.2	10.1	11.7	12.8	12.8	14.2	13.7	13.8	12.9	10.4	9.6
9 - 10	10.8	11.1	10.1	11.7	12.8	12.8	14.2	13.8	13.8	12.9	10.3	9.4
10 - 11	10.1	10.5	9.6	11.3	12.5	12.6	14.1	13.7	13.5	12.2	9.5	8.6
11 - 12	9	9.5	8.6	10.3	11.8	12	13.5	12.9	12.8	11.2	8.5	7.7
12 - 13	8.5	8.8	7.9	9.5	10.9	11	12.5	12.1	12	10.5	7.9	7.3
13 - 14	7.9	8.2	7.2	8.8	10.1	10.3	11.8	11.6	11.4	9.8	7.3	6.9
14 - 15	7.3	7.5	6.6	8	9.4	9.8	11.3	11	10.8	9.2	6.8	6.5
15 - 16	6.7	6.8	6	7.1	8.8	9.2	10.8	10.4	10.2	8.6	6.1	6.1
16 - 17	6.1	6.2	5.5	6.5	8.2	8.8	10.3	9.9	9.7	8.1	5.8	5.8
17 - 18	5.8	5.9	5.3	6.1	8	8.6	10	9.6	9.3	7.7	5.6	5.7
18 - 19	5.8	6	5.2	6	7.8	8.5	9.9	9.5	9.2	7.5	5.6	5.7
19 - 20	6	6.2	5.4	6.3	7.9	8.7	9.9	9.3	9.2	7.7	5.9	5.7
20 - 21	6.5	6.8	5.8	6.8	8.3	8.9	10.1	9.3	9.3	7.9	6.4	6
21 - 22	7.2	7.6	6.5	7.4	8.8	9.2	10.4	9.4	9.6	8.2	7.2	6.3
22 - 23	7.6	8	6.8	7.9	9.2	9.6	10.7	9.8	10	8.5	8.1	6.9
23 - 24	8.1	8.4	7.1	8.4	9.7	10.1	11.4	10.3	10.7	9.1	8.8	7.3

Source: SWERA[75].

Appendix B. Wind turbine models

Table B1–Power functions for wind turbines

Nominal power of wind turbines	Hubheight (m)	R^2_{adj}	Power functions (kW)
2000 kW	108	99.40%	$0.939 - 18.980v^1 + 18.389v^2 - 5.718v^3 + 1.092v^4 - 0.053v^5$ (28)
2300 kW	114	99.90%	$-10.252 + 47.467v^1 - 28.959v^2 + 6.013v^3 - 0.223v^4 - 0.001v^5$ (29)
2300 kW	108	99.92%	$-4.898 + 23.137v^1 - 14.296v^2 + 2.927v^3 + 0.163v^4 - 0.018v^5$ (30)
2350 kW	84	99.92%	$-4.898 + 23.137v^1 - 14.296v^2 + 2.927v^3 + 0.163v^4 - 0.018v^5$ (31)
3000 kW	84	99.98%	$-10.845 + 56.798v^1 - 39.354v^2 + 9.524v^3 - 0.557v^4 + 0.009v^5$ (32)
3050 kW	124	99.94%	$11.084 - 97.144v^1 + 78.550v^2 - 21.207v^3 + 2.867v^4 - 0.120v^5$ (33)
3500 kW	74	99.93%	$-10.797 + 51.616v^1 - 32.958v^2 + 7.236v^3 - 0.077v^4 - 0.014v^5$ (34)
4200 kW	135	99.98%	$-7.636 + 52.374v^1 - 44.998v^2 + 12.780v^3 - 0.489v^4 - 0.008v^5$ (35)
7580 kW	135	99.91%	$-47.652 + 211.978v^1 - 129.195v^2 + 27.331v^3 - 1.489v^4 + 0.022v^5$ (36)

Appendix C. Financial data

Table C1–Assumptions for financial analysis

Parameters	Value	References
Wind investment	R$ 4,315,289.33 per MW installed	CCEE [101]
Solar photovoltaic investment	R$ 4,044,305.06 per MW installed	CCEE [101]
ESS investment cost (current)	R$ 8,000,000.00 per MW installed	Rahman et al. [62], Cole and Frazier [92], Fu et al. [89]
ESS investment cost (ideal)	R$ 2,000,000.00 per MW installed	Penisa et al. [93]
Wind energy price*	R$ 189.00 per MWh	EPE [102]
Solar energy price*	R$ 209.00 per MWh	EPE [102]
Compensation for storage (current)	R$ 0.00 per MWh	ANEEL [20], EPE [19]
Compensation for storage (ideal)**	R$ 380.12 per MWh	Davies et al. [94]
Battery recharge cost***	R$ 49.77 per MWh	CCEE [103]
Annual energy production (kWh)	Calculated for each experimental condition	Equation15
Residual value	10% on investment	Modified from Azevêdo et al.[84]
Depreciation	5% per year	Aquila et al. [38]
Project construction time	2 years	Aquila et al. [38]
Project lifetime	20 years	Aquila et al. [38]
Leasing	1.0 % on investment	Aquila et al. [6]
Operation and Maintenance (O&M) costs for wind energy	2.0 % on investment	Aquila et al. [38]
O&M for solar energy	0.9% on investment	Azevêdo et al. [84]
O&M for ESS	R$ 57,917.77 per MW installed	Rahman et al. [62]
Transmission system usage fee (TSUF)	R$ 4,580.00 per MW installed	Aquila et al. [37]
TSUF discount	0 %	Brazil [104]
Electric Energy Commercialization Chamber Fee (CCEE)	R$ 0.07 per MWh	Aquila et al. [37]
National System Operator (NSO) Fee	R$ 470.00 per MW installed	Aquila et al. [37]
Electric Energy Services Inspection Fee (TFSEE)	R$ 3,058.92per MW installed	MME [105], Brazil [106]
Plant insurance	0.3% on investment	Aquila et al. [37]
Tax: PIS (S*ocial Integration Program*)	3.0 %on investment	Aquila et al. [37]
Tax: COFINS (*Contribution to Social Security Financing*)	0.65% on sales	Aquila et al. [37]
Calculation basis for presumed profit	8.0 % on sales	Modified from Aquila et al. [37]
Corporate Income Tax (IRPJ)	15% on calculation basis + 10% on the value that exceeds R$ 240,000.00	Modified from Aquila et al. [37]
Social Contribution on Net Income (CSLL)	9% on calculation basis	Modified from Aquila et al. [37]
Debt percentage (D)	40.0 %	Aquila et al. [70]
Equity percentage (*E*)	60.0 %	Aquila et al. [70]
Risk-free rate (r_f)	3.07 %	Aquila et al. [70]
Expected market return (r_m)	11.20 %	FGV [107]
$\beta_{unleveraged}$	0,70	Aquila et al. [70]
Debt cost (k_d)	8,08 %	BNDES [108]
Equity cost (k_e)	9,37 %	Equation 28
Broad Consumer Price NationalIndex (IPCA)	4,52 %	IBGE [109]
WACC	7,77 %	Equation 27
Deflated discount rate (*i*)	3,11 %	Equation 30
Exchange rate(R$/US$)	R$ 5,59	Quotation on 04/16/2021

* ceiling price of the 30th new energy auction with a delivery horizon in six years (A-6), realized in 2019.
** considering the possibility of stacking revenues.
*** minimum hourly price for the Northeast submarket until 03/31/2021.

References

[1] M. Mahmoud, M. Ramadan, A.-G. Olabi, K. Pullen, S. Naher, A review of mechanical energy storage systems combined with wind and solar applications, Energy Convers. Manag. 210 (2020) 112670. https://doi.org/10.1016/j.enconman.2020.112670.

[2] IEA - International Energy Agency, Global energy demand rose by 2.3% in 2018, its fastest pace in the last

decade, 2019, (2019).
[3] L.C.S. Rocha, G. Aquila, P. Rotela Junior, A.P. de Paiva, E. de O. Pamplona, P.P. Balestrassi, A stochastic economic viability analysis of residential wind power generation in Brazil, Renew. Sustain. Energy Rev. 90 (2018) 412–419. https://doi.org/10.1016/j.rser.2018.03.078.
[4] E. Marrasso, C. Roselli, M. Sasso, Electric efficiency indicators and carbon dioxide emission factors for power generation by fossil and renewable energy sources on hourly basis, Energy Convers. Manag. 196 (2019) 1369–1384. https://doi.org/10.1016/j.enconman.2019.06.079.
[5] R. Corrêa da Silva, I. de Marchi Neto, S. Silva Seifert, Electricity supply security and the future role of renewable energy sources in Brazil, Renew. Sustain. Energy Rev. 59 (2016) 328–341. https://doi.org/10.1016/j.rser.2016.01.001.
[6] G. Aquila, L.C.S. Rocha, P. Rotela Junior, E. de O. Pamplona, A.R. de Queiroz, A.P. de Paiva, Wind power generation: An impact analysis of incentive strategies for cleaner energy provision in Brazil, J. Clean. Prod. 137 (2016) 1100–1108. https://doi.org/10.1016/j.jclepro.2016.07.207.
[7] G. Aquila, R.S. Peruchi, P. Rotela Junior, L.C.S. Rocha, A.R. de Queiroz, E. de O. Pamplona, P.P. Balestrassi, Analysis of the wind average speed in different Brazilian states using the nested GR&R measurement system, Measurement. 115 (2018) 217–222. https://doi.org/10.1016/j.measurement.2017.10.048.
[8] R.M. Dutra, A.S. Szklo, Incentive policies for promoting wind power production in Brazil: Scenarios for the Alternative Energy Sources Incentive Program (PROINFA) under the New Brazilian electric power sector regulation, Renew. Energy. 33 (2008) 65–76. https://doi.org/10.1016/j.renene.2007.01.013.
[9] P. Rotela Junior, E. Fischetti, V.G. Araújo, R.S. Peruchi, G. Aquila, L.C.S. Rocha, L.S. Lacerda, Wind Power Economic Feasibility under Uncertainty and the Application of ANN in Sensitivity Analysis, Energies. 12 (2019) 2281. https://doi.org/10.3390/en12122281.
[10] J. Schmidt, R. Cancella, A.O. Pereira, An optimal mix of solar PV, wind and hydro power for a low-carbon electricity supply in Brazil, Renew. Energy. 85 (2016) 137–147. https://doi.org/10.1016/j.renene.2015.06.010.
[11] EPE – Empresa de Pesquisa Energética, Avaliação da geração de usinas híbridas eólico-fotovoltaicas: Proposta metodológica e estudos de caso, (2017). https://www.epe.gov.br/sites-pt/publicacoes-dados-abertos/publicacoes/PublicacoesArquivos/publicacao-232/topico-214/Metodologia para avaliação de usinas híbridas eólico-fotovoltaicas.pdf (accessed April 15, 2021).
[12] M. de Falco, N. Mastrandrea, An Analytical Model for Optimizing the Combination of Energy Sources in a Single Power Transmission Network, J. Renew. Energy. 2014 (2014) 1–10. https://doi.org/10.1155/2014/143736.
[13] T. Weitzel, C.H. Glock, Energy management for stationary electric energy storage systems: A systematic literature review, Eur. J. Oper. Res. 264 (2018) 582–606. https://doi.org/10.1016/j.ejor.2017.06.052.
[14] P.P. Biswas, P.N. Suganthan, G.A.J. Amaratunga, Optimal power flow solutions incorporating stochastic wind and solar power, Energy Convers. Manag. 148 (2017) 1194–1207. https://doi.org/10.1016/j.enconman.2017.06.071.
[15] M. Götz, J. Lefebvre, F. Mörs, A. McDaniel Koch, F. Graf, S. Bajohr, R. Reimert, T. Kolb, Renewable Power-to-Gas: A technological and economic review, Renew. Energy. 85 (2016) 1371–1390. https://doi.org/10.1016/j.renene.2015.07.066.
[16] J. Münderlein, M. Steinhoff, S. Zurmühlen, D.U. Sauer, Analysis and evaluation of operations strategies based on a large scale 5 MW and 5 MWh battery storage system, J. Energy Storage. 24 (2019) 100778. https://doi.org/10.1016/j.est.2019.100778.
[17] A.O. Gbadegesin, Y. Sun, N.I. Nwulu, Techno-economic analysis of storage degradation effect on levelised cost of hybrid energy storage systems, Sustain. Energy Technol. Assessments. 36 (2019) 100536. https://doi.org/10.1016/j.seta.2019.100536.
[18] D. Kucevic, B. Tepe, S. Englberger, A. Parlikar, M. Mühlbauer, O. Bohlen, A. Jossen, H. Hesse, Standard battery energy storage system profiles: Analysis of various applications for stationary energy storage systems using a holistic simulation framework, J. Energy Storage. 28 (2020) 101077. https://doi.org/10.1016/j.est.2019.101077.
[19] EPE – Empresa de Pesquisa Energética, Sistemas de Armazenamento em Baterias: Aplicações e Questões Relevantes para o Planejamento, (2019). https://www.epe.gov.br/pt/publicacoes-dados-abertos/publicacoes/nt-sistemas-de-armazenamento-em-baterias-aplicacoes-e-questoes-relevantes-para-o-planejamento (accessed April 15, 2021).
[20] ANEEL – Agência Nacional de Energia Elétrica, Nota Técnica nº 094/2020–SRG/ANEEL, 2020, (2020). https://www.aneel.gov.br/tomadas-de-subsidios?p_p_id=participacaopublica_WAR_participacaopublicaportlet&p_p_lifecycle=2&p_p_state=normal&p_p_mode=view&p_p_cacheability=cacheLevelPage&p_p_col_id=column-2&p_p_col_count=1&_participacaopublica_WAR_participaca (accessed October 16, 2020).
[21] C.K. Das, O. Bass, G. Kothapalli, T.S. Mahmoud, D. Habibi, Overview of energy storage systems in distribution networks: Placement, sizing, operation, and power quality, Renew. Sustain. Energy Rev. 91 (2018) 1205–1230. https://doi.org/10.1016/j.rser.2018.03.068.
[22] J. Münderlein, G. Ipers, M. Steinhoff, S. Zurmühlen, D.U. Sauer, Optimization of a hybrid storage system and

evaluation of operation strategies, Int. J. Electr. Power Energy Syst. 119 (2020) 105887. https://doi.org/10.1016/j.ijepes.2020.105887.

[23] O. Schmidt, S. Melchior, A. Hawkes, I. Staffell, Projecting the Future Levelized Cost of Electricity Storage Technologies, Joule. 3 (2019) 81–100. https://doi.org/10.1016/j.joule.2018.12.008.

[24] Y.J. Zhang, C. Zhao, W. Tang, S.H. Low, Profit-Maximizing Planning and Control of Battery Energy Storage Systems for Primary Frequency Control, IEEE Trans. Smart Grid. 9 (2018) 712–723. https://doi.org/10.1109/TSG.2016.2562672.

[25] V. Silvera, D.A. Cantane, R. Reginatto, J.J.G. Ledesma, M.H. Schimdt, O.H. Ando Junior, Energy Storage Technologies towards Brazilian Electrical System, Renew. Energy Power Qual. J. 1 (2018) 380–386. https://doi.org/10.24084/repqj16.319.

[26] G.L. Kyriakopoulos, G. Arabatzis, Electrical energy storage systems in electricity generation: Energy policies, innovative technologies, and regulatory regimes, Renew. Sustain. Energy Rev. 56 (2016) 1044–1067. https://doi.org/10.1016/j.rser.2015.12.046.

[27] IRENA - International Renewable Energy Agency, Utility-Scale Batteries: Innovation Landscape Brief, (2019).

[28] M.Y. Haller, D. Carbonell, M. Dudita, D. Zenhäusern, A. Häberle, Seasonal energy storage in aluminium for 100 percent solar heat and electricity supply, Energy Convers. Manag. X. 5 (2020) 100017. https://doi.org/10.1016/j.ecmx.2019.100017.

[29] O. Schmidt, A. Hawkes, A. Gambhir, I. Staffell, The future cost of electrical energy storage based on experience rates, Nat. Energy. 2 (2017) 17110. https://doi.org/10.1038/nenergy.2017.110.

[30] W. Cole, A.W. Frazier, Cost Projections for Utility-Scale Battery Storage. Golden, CO: National Renewable Energy Laboratory. NREL/TP-6A20-73222, (2019). https://www.nrel.gov/docs/fy19osti/73222.pdf (accessed August 4, 2020).

[31] G.G. Dranka, P. Ferreira, Towards a smart grid power system in Brazil: Challenges and opportunities, Energy Policy. 136 (2020) 111033. https://doi.org/10.1016/j.enpol.2019.111033.

[32] L.S. Lacerda, P.R. Junior, R.S. Peruchi, G. Chicco, L.C.S. Rocha, G. Aquila, L.M.C. Junior, Microgeneration of Wind Energy for Micro and Small Businesses: Application of ANN in Sensitivity Analysis for Stochastic Economic Feasibility, IEEE Access. 8 (2020) 73931–73946. https://doi.org/10.1109/ACCESS.2020.2988593.

[33] L.C.S. Rocha, G. Aquila, E. de O. Pamplona, A.P. de Paiva, B.G. Chieregatti, J. de S.B. Lima, Photovoltaic electricity production in Brazil: A stochastic economic viability analysis for small systems in the face of net metering and tax incentives, J. Clean. Prod. 168 (2017) 1448–1462. https://doi.org/10.1016/j.jclepro.2017.09.018.

[34] S.B. Silva, M.M. Severino, M.A.G. de Oliveira, A stand-alone hybrid photovoltaic, fuel cell and battery system: A case study of Tocantins, Brazil, Renew. Energy. 57 (2013) 384–389. https://doi.org/10.1016/j.renene.2013.02.004.

[35] M. Nunes Fonseca, E. de Oliveira Pamplona, A.R. de Queiroz, V.E. de Mello Valerio, G. Aquila, S. Ribeiro Silva, Multi-objective optimization applied for designing hybrid power generation systems in isolated networks, Sol. Energy. 161 (2018) 207–219. https://doi.org/10.1016/j.solener.2017.12.046.

[36] G. Aquila, A.R. de Queiroz, P.P. Balestrassi, P. Rotella Junior, L.C.S. Rocha, E.O. Pamplona, W.T. Nakamura, Wind energy investments facing uncertainties in the Brazilian electricity spot market: A real options approach, Sustain. Energy Technol. Assessments. 42 (2020) 100876. https://doi.org/10.1016/j.seta.2020.100876.

[37] G. Aquila, L.C. Souza Rocha, P. Rotela Junior, J.Y. Saab Junior, J. de Sá Brasil Lima, P.P. Balestrassi, Economic planning of wind farms from a NBI-RSM-DEA multiobjective programming, Renew. Energy. 158 (2020) 628–641. https://doi.org/10.1016/j.renene.2020.05.179.

[38] G. Aquila, L.C. Souza Rocha, E. de Oliveira Pamplona, A.R. de Queiroz, P. Rotela Junior, P.P. Balestrassi, M.N. Fonseca, Proposed method for contracting of wind-photovoltaic projects connected to the Brazilian electric system using multiobjective programming, Renew. Sustain. Energy Rev. 97 (2018) 377–389. https://doi.org/10.1016/j.rser.2018.08.054.

[39] G. Aquila, A.R. de Queiroz, P. Rotela Junior, L.C.S. Rocha, E. de O. Pamplona, P.P. Balestrassi, Contribution for bidding of wind-photovoltaic on grid farms based on NBI-EFA-SNR method, Sustain. Energy Technol. Assessments. 40 (2020) 100754. https://doi.org/10.1016/j.seta.2020.100754.

[40] A. Durusu, A. Erduman, An Improved Methodology to Design Large-Scale Photovoltaic Power Plant, J. Sol. Energy Eng. 140 (2018). https://doi.org/10.1115/1.4038589.

[41] K. Miettinen, Nonlinear Multiobjective Optimization, Springer US, Boston, MA, 1998. https://doi.org/10.1007/978-1-4615-5563-6.

[42] L.C.S. Rocha, P. Rotela Junior, G. Aquila, A.P. de Paiva, P.P. Balestrassi, Toward a robust optimal point selection: a multiple-criteria decision-making process applied to multi-objective optimization using response surface methodology, Eng. Comput. 37 (2021) 2735–2761. https://doi.org/10.1007/s00366-020-00973-5.

[43] A. Abdelkader, A. Rabeh, D. Mohamed Ali, J. Mohamed, Multi-objective genetic algorithm based sizing optimization of a stand-alone wind/PV power supply system with enhanced battery/supercapacitor hybrid energy storage, Energy. 163 (2018) 351–363. https://doi.org/10.1016/j.energy.2018.08.135.

[44] N. Yin, R. Abbassi, H. Jerbi, A. Rezvani, M. Müller, A day-ahead joint energy management and battery sizing

framework based on θ-modified krill herd algorithm for a renewable energy-integrated microgrid, J. Clean. Prod. 282 (2021) 124435. https://doi.org/10.1016/j.jclepro.2020.124435.

[45] S. Tang, M. Jiang, R. Abbassi, H. Jerbi, M. Latifi, A cost-oriented resource scheduling of a solar-powered microgrid by using the hybrid crow and pattern search algorithm, J. Clean. Prod. 313 (2021) 127853. https://doi.org/10.1016/j.jclepro.2021.127853.

[46] L. Zhao, H. Jerbi, R. Abbassi, B. Liu, M. Latifi, H. Nakamura, Sizing renewable energy systems with energy storage systems based microgrids for cost minimization using hybrid shuffled frog-leaping and pattern search algorithm, Sustain. Cities Soc. 73 (2021) 103124. https://doi.org/10.1016/j.scs.2021.103124.

[47] C.E. Shannon, A Mathematical Theory of Communication, Bell Syst. Tech. J. 27 (1948) 379–423. https://doi.org/10.1002/j.1538-7305.1948.tb01338.x.

[48] P. Grünewald, T. Cockerill, M. Contestabile, P. Pearson, The role of large scale storage in a GB low carbon energy future: Issues and policy challenges, Energy Policy. 39 (2011) 4807–4815. https://doi.org/10.1016/j.enpol.2011.06.040.

[49] S. Ruester, J. Vasconcelos, X. He, E. Chong, J.M. Glachant, Electricity Storage: How to Facilitate its Deployment and Operation in the EU, Policy Br. (2012). https://doi.org/10.2870/41627.

[50] J. Cornell, Experiments with mixtures: designs, models, and the analysis of mixture data., 3rd ed., John Wiley & Sons Inc, New York, 2002.

[51] D.C. Montgomery, Design and Analysis of Experiments, John Wiley & Sons Inc, New York, 2009.

[52] R.H. Myers, D.C. Montgomery, C.M. Anderson-Cook, Response Surface Methodology: process and product optimization using designed experiments, 3rd ed., John Wiley & Sons Inc, New York, 2009.

[53] V. Oree, S.Z. Sayed Hassen, P.J. Fleming, Generation expansion planning optimisation with renewable energy integration: A review, Renew. Sustain. Energy Rev. 69 (2017) 790–803. https://doi.org/10.1016/j.rser.2016.11.120.

[54] L.C.S. Rocha, A.P. de Paiva, P. Rotela Junior, P.P. Balestrassi, P.H. da Silva Campos, Robust multiple criteria decision making applied to optimization of AISI H13 hardened steel turning with PCBN wiper tool, Int. J. Adv. Manuf. Technol. 89 (2017) 2251–2268. https://doi.org/10.1007/s00170-016-9250-8.

[55] I. Das, J.E. Dennis, A closer look at drawbacks of minimizing weighted sums of objectives for Pareto set generation in multicriteria optimization problems, Struct. Optim. 14 (1997) 63–69. https://doi.org/10.1007/BF01197559.

[56] I. Das, J.E. Dennis, Normal-Boundary Intersection: A New Method for Generating the Pareto Surface in Nonlinear Multicriteria Optimization Problems, SIAM J. Optim. 8 (1998) 631–657. https://doi.org/10.1137/S1052623496307510.

[57] L.C.S. Rocha, A.P. de Paiva, P.P. Balestrassi, G. Severino, P. Rotela Junior, Entropy-Based Weighting for Multiobjective Optimization: An Application on Vertical Turning, Math. Probl. Eng. 2015 (2015) 1–11. https://doi.org/10.1155/2015/608325.

[58] L.C.S. Rocha, A.P. de Paiva, P.P. Balestrassi, G. Severino, P. Rotela Junior, Entropy-Based weighting applied to normal boundary intersection approach: the vertical turning of martensitic gray cast iron piston rings case, Acta Sci. Technol. 37 (2015) 361. https://doi.org/10.4025/actascitechnol.v37i4.27819.

[59] L.C.S. Rocha, A.P. de Paiva, P. Rotela Junior, P.P. Balestrassi, P.H. da Silva Campos, J.P. Davim, Robust weighting applied to optimization of AISI H13 hardened-steel turning process with ceramic wiper tool: A diversity-based approach, Precis. Eng. 50 (2017) 235–247. https://doi.org/10.1016/j.precisioneng.2017.05.011.

[60] R. Navabi, S. Abedi, S.H. Hosseinian, R. Pal, On the fast convergence modeling and accurate calculation of PV output energy for operation and planning studies, Energy Convers. Manag. 89 (2015) 497–506. https://doi.org/10.1016/j.enconman.2014.09.070.

[61] M. Brower, Wind Resource Assessment: A Practical Guide to Developing a Wind Project, John Wiley & Sons Inc, United States, 2012.

[62] M.M. Rahman, A.O. Oni, E. Gemechu, A. Kumar, The development of techno-economic models for the assessment of utility-scale electro-chemical battery storage systems, Appl. Energy. 283 (2021) 116343. https://doi.org/10.1016/j.apenergy.2020.116343.

[63] A. Swingler, M. Hall, Initial Comparison of Lithium Battery and High-Temperature Thermal-Turbine Electricity Storage for 100% Wind and Solar Electricity Supply on Prince Edward Island, Energies. 11 (2018) 3470. https://doi.org/10.3390/en11123470.

[64] A. Chadly, E. Azar, M. Maalouf, A. Mayyas, Techno-economic analysis of energy storage systems using reversible fuel cells and rechargeable batteries in green buildings, Energy. 247 (2022) 123466. https://doi.org/10.1016/j.energy.2022.123466.

[65] A.-I. Stroe, J. Meng, D.-I. Stroe, M. Świerczyński, R. Teodorescu, S. Kær, Influence of Battery Parametric Uncertainties on the State-of-Charge Estimation of Lithium Titanate Oxide-Based Batteries, Energies. 11 (2018) 795. https://doi.org/10.3390/en11040795.

[66] A. Stirling, Diversity and ignorance in electricity supply investment, Energy Policy. 22 (1994) 195–216. https://doi.org/10.1016/0301-4215(94)90159-7.

[67] A. Stirling, A general framework for analysing diversity in science, technology and society, J. R. Soc. Interface. 4 (2007) 707–719. https://doi.org/10.1098/rsif.2007.0213.
[68] A. Stirling, Multicriteria diversity analysis, Energy Policy. 38 (2010) 1622–1634. https://doi.org/10.1016/j.enpol.2009.02.023.
[69] W.F. Sharpe, CAPITAL ASSET PRICES: A THEORY OF MARKET EQUILIBRIUM UNDER CONDITIONS OF RISK*, J. Finance. 19 (1964) 425–442. https://doi.org/10.1111/j.1540-6261.1964.tb02865.x.
[70] G. Aquila, W.T. Nakamura, P.R. Junior, L.C. Souza Rocha, E. de Oliveira Pamplona, Perspectives under uncertainties and risk in wind farms investments based on Omega-LCOE approach: An analysis in São Paulo state, Brazil, Renew. Sustain. Energy Rev. 141 (2021) 110805. https://doi.org/10.1016/j.rser.2021.110805.
[71] C. Stetter, J.-H. Piel, J.F.H. Hamann, M.H. Breitner, Competitive and risk-adequate auction bids for onshore wind projects in Germany, Energy Econ. 90 (2020) 104849. https://doi.org/10.1016/j.eneco.2020.104849.
[72] B. Steffen, Estimating the cost of capital for renewable energy projects, Energy Econ. 88 (2020) 104783. https://doi.org/10.1016/j.eneco.2020.104783.
[73] A. Damodaran, Investment Valuation: Tools and Techniques for Determining the Value of Any Asset, 3rd ed., John Wiley & Sons Inc, New York, 2012.
[74] S.A. Ross, R.W. Westerfield, J.F. Jaffe, Administração Financeira: Corporate Finance, 2nd ed., São Paulo, 2002.
[75] SWERA - Solar and Wind Energy Resource Assessment, Global Solar Atlas, (2021). https://openei.org/wiki/Solar_and_Wind_Energy_Resource_Assessment_(SWERA) (accessed April 20, 2021).
[76] INPE - Instituto Nacional de Pesquisas Espaciais, Dados históricos, (2021). http://sinda.crn.inpe.br/PCD/SITE/novo/site/index.php (accessed April 20, 2021).
[77] YINGLI ENERGY, YGE 72 CELL SERIES 2, (2020).
[78] WOBBEN WINDPOWER, Linha de produtos ENERCON, (2015). http://www.wobben.com.br/fileadmin/user_upload/ec_product_br.pdf (accessed March 31, 2021).
[79] M. Hiremath, K. Derendorf, T. Vogt, Comparative Life Cycle Assessment of Battery Storage Systems for Stationary Applications, Environ. Sci. Technol. 49 (2015) 4825–4833. https://doi.org/10.1021/es504572q.
[80] G. Albright, J. Edie, S. Al-Hallaj, A Comparison of Lead Acid to Lithium-ion in Stationary Storage Applications, AllCell Technol. LLC. (2012). https://www.batterypoweronline.com/wp-content/uploads/2012/07/Lead-acid-white-paper.pdf.
[81] S. Eckroad, I. Gyuk, EPRI-DOE handbook of energy storage for transmission & distribution applications. Electric Power Research Institute, Inc., (2003).
[82] K. Mallon, F. Assadian, B. Fu, Analysis of On-Board Photovoltaics for a Battery Electric Bus and Their Impact on Battery Lifespan, Energies. 10 (2017) 943. https://doi.org/10.3390/en10070943.
[83] I. Staffell, R. Green, How does wind farm performance decline with age?, Renew. Energy. 66 (2014) 775–786. https://doi.org/10.1016/j.renene.2013.10.041.
[84] R. de Oliveira Azevêdo, P. Rotela Junior, L.C.S. Rocha, G. Chicco, G. Aquila, R.S. Peruchi, Identification and Analysis of Impact Factors on the Economic Feasibility of Photovoltaic Energy Investments, Sustainability. 12 (2020) 7173. https://doi.org/10.3390/su12177173.
[85] K. Mongird, V.V. Viswanathan, P.J. Balducci, M.J.E. Alam, V. Fotedar, V.S. Koritarov, B. Hadjerioua, Energy storage technology and cost characterization report. Pacific Northwest National Lab.(PNNL), Richland, WA (United States), (2019).
[86] R.R. Hernandez, M.K. Hoffacker, C.B. Field, Land-Use Efficiency of Big Solar, Environ. Sci. Technol. 48 (2014) 1315–1323. https://doi.org/10.1021/es4043726.
[87] A.B. Lovins, Renewable Energy's 'Footprint' Myth, Electr. J. 24 (2011) 40–47. https://doi.org/10.1016/j.tej.2011.06.005.
[88] P. Denholm, M. Hand, M. Jackson, S. Ong, Land Use Requirements of Modern Wind Power Plants in the United States, Golden, CO (United States), 2009. https://doi.org/10.2172/964608.
[89] R. Fu, T.W. Remo, R.M. Margolis, 2018 US utility-scale photovoltaics-plus-energy storage system costs benchmark. National Renewable Energy Lab.(NREL), Golden, CO (United States), (2018). https://www.nrel.gov/docs/fy19osti/71714.pdf (accessed April 8, 2021).
[90] ONS - Operador Nacional do Sistema Elétrico, Boletim Mensal de Geração Solar Fotovoltaica, (2021). http://www.ons.org.br/AcervoDigitalDocumentosEPublicacoes/Boletim Mensal de Geração Solar 2021-02.pdf (accessed April 9, 2021).
[91] ONS - Operador Nacional do Sistema Elétrico, Boletim Mensal de Geração Eólica. Março/2021, (2021). http://www.ons.org.br/AcervoDigitalDocumentosEPublicacoes/Boletim Mensal de Geração Eólica 2021-03.pdf (accessed April 9, 2021).
[92] W. Cole, A.W. Frazier, Cost projections for utility-scale battery storage: 2020 update. Golden, CO: National Renewable Energy Laboratory. NREL/TP-6A20-75385, (2020).
[93] X.N. Penisa, M.T. Castro, J.D.A. Pascasio, E.A. Esparcia, O. Schmidt, J.D. Ocon, Projecting the Price of Lithium-Ion NMC Battery Packs Using a Multifactor Learning Curve Model, Energies. 13 (2020) 5276. https://doi.org/10.3390/en13205276.

[94] D.M. Davies, M.G. Verde, O. Mnyshenko, Y.R. Chen, R. Rajeev, Y.S. Meng, G. Elliott, Combined economic and technological evaluation of battery energy storage for grid applications, Nat. Energy. 4 (2019) 42–50. https://doi.org/10.1038/s41560-018-0290-1.

[95] M.S. Rocha, L.C.S. Rocha, M.B. da S. Feijó, P.L.L. dos S. Marotta, S.C. Mourão, Multiobjective optimization of the flaxseed mucilage extraction process using normal-boundary intersection approach, Br. Food J. ahead-of-p (2021). https://doi.org/10.1108/BFJ-06-2020-0501.

[96] W. Shen, X. Chen, J. Qiu, J.A. Hayward, S. Sayeef, P. Osman, K. Meng, Z.Y. Dong, A comprehensive review of variable renewable energy levelized cost of electricity, Renew. Sustain. Energy Rev. 133 (2020) 110301. https://doi.org/10.1016/j.rser.2020.110301.

[97] IRENA - International Renewable Energy Agency, Renewable power generation costs in 2020, (2021). https://www.irena.org/publications/2021/Jun/Renewable-Power-Costs-in-2020 (accessed April 9, 2020).

[98] I. Pérez-Arriaga, C. Knittel, Utility of the Future: An MIT Energy Initiative response to an industry in transition. Cambridge: MIT, (2016). https://energy.mit.edu/wp-content/uploads/2016/12/Utility-of-the-Future-Full-Report.pdf (accessed August 4, 2020).

[99] G. De Vivero-Serrano, K. Bruninx, E. Delarue, Implications of bid structures on the offering strategies of merchant energy storage systems, Appl. Energy. 251 (2019) 113375. https://doi.org/10.1016/j.apenergy.2019.113375.

[100] K. Afgouni, J.H. Silva Sá, Lithium ore in Brazil, Energy. 3 (1978) 247–253. https://doi.org/10.1016/0360-5442(78)90020-8.

[101] CCEE - Câmara de Comercialização de Energia Elétrica, Resultado consolidado dos leilões - 03/2021, (2021). https://www.ccee.org.br/portal/faces/acesso_rapido_header_publico_nao_logado/biblioteca_virtual?tipo=Resultado Consolidado&assunto=Leilão&_afrLoop=235659826591863&_adf.ctrl-state=n14wd9set_54#!%40%40%3F_afrLoop%3D235659826591863%26tipo%3DResultado%2BConso (accessed April 15, 2021).

[102] EPE – Empresa de Pesquisa Energética, Leilões de Energia Elétrica de 2019: Apresentando os resultados e avaliando os caminhos do planejamento energético, (2019). https://www.epe.gov.br/sites-pt/publicacoes-dados-abertos/publicacoes/PublicacoesArquivos/publicacao-451/Informe Leilões 2019_v3.pdf (accessed April 15, 2021).

[103] CCEE - Câmara de Comercialização de Energia Elétrica, Lista de preços horários até 31/03/2021, (2021). https://www.ccee.org.br/portal/faces/preco_horario_veja_tambem/preco_horario?_adf.ctrl-state=grwj51se_1&_afrLoop=112037815897725#!%40%40%3F_afrLoop%3D112037815897725%26_adf.ctrl-state%3Dgrwj51se_5 (accessed April 15, 2021).

[104] BRAZIL, Lei nº 14.120, de 1º de março de 2021. Altera a Lei nº 9.991, de 24 de julho de 2000, a Lei nº 5.655, de20 de maio de 1971, a Lei nº 9.427, de 26 de dezembro de 1996,a Lei nº 10.438, de 26 de abril de 2002, a Lei nº 10.848, de 15 demarço de 2004, a Lei nº, (2021). https://www.in.gov.br/en/web/dou/-/lei-n-14.120-de-1-de-marco-de-2021-306116199 (accessed April 16, 2021).

[105] MME - Ministério de Minas e Energia, Retificação. Diário Oficial da União, seção 1, nº 6, de 9 de janeiro de 2020, 2020.

[106] BRAZIL, Lei nº 12.783, de 11 de janeiro de 2013. Dispõe sobre as concessões degeração, transmissão e distribuição de energia elétrica, sobre a redução dosencargos setoriais e sobre a modicidade tarifária; altera as Leis nos 10.438, de 26 deabril de 2002, 12.111, (2013). http://www.planalto.gov.br/ccivil_03/_ato2011-2014/2013/lei/L12783.htm (accessed April 15, 2021).

[107] FGV - Fundação Getúlio Vargas, Série de equity risk premium, (2021). https://ceqef.fgv.br/node/594 (accessed April 14, 2021).

[108] BNDES - Banco Nacional de Desenvolvimento Econômico e Social, BNDES Finem - Geração de energia, (2021). https://www.bndes.gov.br/wps/portal/site/home/financiamento/produto/bndes-finem-energia (accessed April 14, 2021).

[109] IBGE - Instituto Brasileiro de Geografia e Estatística, Índice Nacional de Preços ao Consumidor Amplo - IPCA, (2021). https://www.ibge.gov.br/estatisticas/economicas/precos-e-custos/9256-indice-nacional-de-precos-ao-consumidor-amplo.html?=&t=series-historicas (accessed April 14, 2021).